Bioorganic & Medicinal Chemistry 21 (2013) 2319–2332

Contents lists available at SciVerse ScienceDirect

Bioorganic & Medicinal Chemistry

journal homepage: www.elsevier.com/locate/bmc

Design and synthesis of a series of α-benzyl phenylpropanoic acid-type peroxisome proliferator-activated receptor (PPAR) gamma partial agonists with improved aqueous solubility

Masao Ohashi [a], Takuji Oyama [b], Endy Widya Putranto [c], Tsuyoshi Waku [d], Hiromi Nobusada [a], Ken Kataoka [e], Kenji Matsuno [a], Masakazu Yashiro [f], Kosuke Morikawa [g,†], Nam-ho Huh [c], Hiroyuki Miyachi [a,*]

[a] Graduate School of Medicine, Dentistry and Pharmaceutical Sciences, Okayama University, 1-1-1 Tsushima-Naka, Kita-ku, Okayama 700-8530, Japan
[b] Department of Biotechnology, Faculty of Life and Environmental Sciences, University of Yamanashi, 4-4-37 Takeda, Kofu City, Yamanashi 400-8510, Japan
[c] Department of Cell Biology, Okayama University, Graduate School of Medicine, Dentistry and Pharmaceutical Sciences, 2-5-1 Shikatacho, Kita-ku, Okayama 700-8558, Japan
[d] Graduate School of Pharmaceutical Sciences, University of Tokyo, Hongo, Bunkyo-ku, Tokyo 113-0033, Japan
[e] Department of Life Science, Faculty of Science, Okayama University of Science, 1-1 Ridai-cho, Kita-ku, Okayama 700-0005, Japan
[f] Department of Surgical Oncology, Osaka City University, Graduate School of Medicine, 1-4-3 Asahimachi, Abeno-ku, Osaka 545-8585, Japan
[g] Institute for Protein Research, Osaka University, 6-2-3 Furuedai, Suita, Osaka 565-0874, Japan

ARTICLE INFO

Article history:
Received 26 December 2012
Revised 2 February 2013
Accepted 4 February 2013
Available online 14 February 2013

Keywords:
Human peroxisome proliferator-activated receptor
PPAR gamma
Partial agonist
Structural biology

ABSTRACT

In the continuing study directed toward the development of peroxisome proliferator-activated receptor gamma (hPPARγ) agonist, we attempted to improve the water solubility of our previously developed hPPARγ-selective agonist **3**, which is insufficiently soluble for practical use, by employing two strategies: introducing substituents to reduce its molecular planarity and decreasing its hydrophobicity via replacement of the adamantyl group with a heteroaromatic ring. The first approach proved ineffective, but the second was productive. Here, we report the design and synthesis of a series of α-benzyl phenylpropanoic acid-type hPPARγ partial agonists with improved aqueous solubility. Among them, we selected (***R***)-**7j**, which activates hPPARγ to the extent of about 65% of the maximum observed with a full agonist, for further evaluation. The ligand-binding mode and the reason for the partial-agonistic activity are discussed based on X-ray-determined structure of the complex of hPPARγ ligand-binding domain (LBD) and (***R***)-**7j** with previously reported ligand-LDB structures. Preliminal apoptotic effect of (***R***)-**7j** against human scirrhous gastric cancer cell line OCUM-2MD3 is also described.

1. Introduction

Peroxisome proliferator-activated receptor γ (hPPARγ) is the most extensively investigated subtype among the three hPPAR subtypes, hPPARα, hPPARδ and PPARγ. It is expressed abundantly in adipose tissue and macrophages,[1] and is up-regulated in various types of cancer cells.[2,3] hPPARγ is a master regulator of fatty acid and glucose homeostasis,[4–6] but also has a range of other activities.[7–10] Some hPPARγ ligands, such as pioglitazone (**1**) have been reported to induce cell differentiation and apoptosis in malignant tumor cells,[11] and hPPARγ ligands may have potential as anticancer agents. We are interested in the potential application of hPPARγ ligands to treat scirrhous gastric cancer, which has a poor survival rate of less than 20%.[12,13]

We have extensively studied the structural design and synthesis of subtype-selective hPPAR ligands based on phenylpropanoic acid as a scaffold. We have successfully created a series of α-substituted phenylpropanoic acid-type hPPARα-selective agonists,[14,15] a hPPARαδ dual agonist (TIPP-401),[16,17] a hPPARδ-selective agonist (TIPP-204),[18] and a hPPAR αδγ pan agonist (TIPP-703 (**2**)).[19] Furthermore, we recently reported a hPPARγ-selective agonist (MEKT-1 (**3**)), which was designed on the basis of a comparative X-ray crystallographic analysis of **3** complexed with the hPPARγ ligand binding domain (LBD) (Fig. 1).[20]

Although **3** exhibited potent, hPPARγ-selective in vitro transactivation activity, its aqueous solubility is very poor. Therefore, for

Abbreviations: NR, nuclear receptor; hPPAR, human peroxisome proliferator-activated receptor; LBD, ligand-binding domain; PDB, protein data bank.

* Corresponding author. Tel.: +81 086 251 7930.
E-mail address: miyachi@pharm.okayama-u.ac.jp (H. Miyachi).
† Present address: International Institute for Advanced Studies 9-3, Kizugawadai, Kizugawa City, Kyoto 619-0225, Japan.

0968-0896/$ - see front matter © 2013 Elsevier Ltd. All rights reserved.
http://dx.doi.org/10.1016/j.bmc.2013.02.003

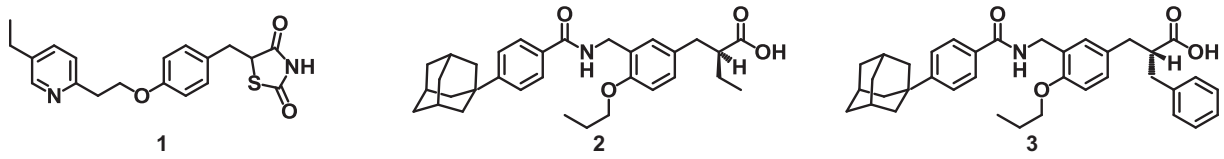

Figure 1. The chemical structures of pioglitazone (**1**) and our hPPARγ agonists **2** and **3**.

in vivo evaluation studies, it was necessary to improve the solubility of **3**. Here, we report the design, synthesis and in vitro pharmacological evaluation of a series of α-benzyl phenylpropanoic acid-type hPPARγ-selective partial agonists with improved aqueous solubility, as candidate anti-scirrhous gastric cancer agents. We also discuss the binding mode of these compounds and the reason why they exhibit partial agonistic activity, based a comparison of the X-ray-determined structures of ligand complexes with the hPPARγ ligand binding site.

2. Experimental design

2.1. Chemistry

The synthesis of the present series of compounds is illustrated in Scheme 1 (routes 1, 2). Compounds (***R***)-**7a**–(***R***)-**7c** and (***R***)-**7e** were prepared according to reported methods, by amide-alkylation[21] of the formyl derivative **6** with the corresponding benzamides, followed by LiOOH hydrolysis (route 1).

Compounds (***R***)-**7d** and (***R***)-**7f**–(***R***)-**7l** were prepared from **6** by an alternative method (route 2). Compound **6** was treated with hydroxylamine HCl, and subsequent reduction with 10% Pd on carbon afforded aminomethylbenzene derivative **9** as the hydrochloric acid salt. Compound **9** was treated with the appropriate benzoic acid derivatives in the presence of the condensing agent, and subsequent hydrolysis with LiOOH afforded the desired compounds.

2.2. Hydrophobicity assessment with HPLC

Reversed-phase HPLC analyses were performed on an analytical column (PegasilODS SP100 column (4.6 mm × 150 mm; flow rate of 1 mL/min; solvent, MeCN/0.1% TFA = 3:1 v/v; detection at 254 nm or 296 nm).

2.3. Thermodynamic aqueous solubility

Thermodynamic solubility determination was based on the method of Avdeef and Testa.[22] The concentration of sample solution was calculated using a previously determined calibration curve, corrected for the dilution factor of the sample.

2.4. Transient transfection assays

The African green monkey kidney cell line CV-1 was used for the transfection assay. CV-1 cells were seeded in 24-well plates and cultured for 24 h. The transfection mixtures were added to the cells and the plates were incubated for 5 h according to the manufacturer's instructions. After the transfection, incubation was continued for an additional 40 h in the presence of the assay compounds or reference compounds. Cell lysates were prepared with a lysis buffer and used in the luciferase and βGAL assays. Luciferase and βGAL activities were measured according to the methods of Umesono et al.,[23] with slight modifications. A substrate reagent kit (Picagene, Toyo Ink) was used for the luciferase assay.

2.5. Expression, purification, and crystallization

Human PPARγ LBD (residues 203–477) was prepared as previously described,[24] that is, recombinant hPPARγ LBD was expressed as an N-terminal His-tagged protein in *Escherichia coli* BL21 (DE3), using the pET28a vector (Novagen). The protein was purified by means of several steps of column chromatography (His-Trap HP column (GE Healthcare), HiPrep 26/10 desalting column (GE

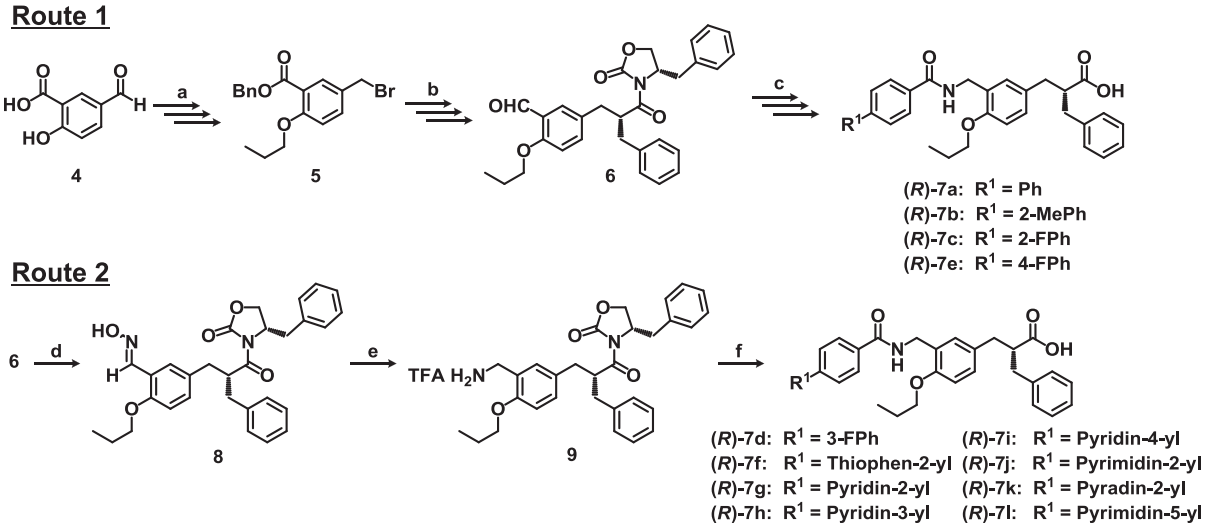

Scheme 1. Synthetic route to the present series of compounds. Reagents and conditions: (a) (1) BnBr, $KHCO_3$, DMF, rt, overnight, quant.; (2) *n*PrI, K_2CO_3, DMF, 60 °C, overnight, quant.; (3) $NaBH_4$, EtOH, rt 2 h, 91%; (4) PBr_3, diethylether, 0 °C, 1.5 h, 52%; (b) (1) (***R***)-3-(3-phenylpropanoyl)-4-benzyloxazolidin-2-one, LiHMDS, dehydrated THF, −50 to 0 °C, 2 h, 64%; (2) H_2, 10% Pd-C, AcOEt, rt, 3 h, 55%; (3) BH_3–THF, dehydrated THF, 0 °C, overnight; (4) activated MnO_2, CH_2Cl_2, rt, overnight, 65% (2 steps); (c) (1) benzamide derivative, triethylsilane, TFA, toluene, reflux, 48 h, 97%; (2) LiOH–H_2O, 30% H_2O_2, THF/H_2O = 4:1 (v/v), 0 °C, 2.5 h then rt 3 h, 86%; (d) hydroxylamine HCl, pyridine, ethanol, reflux, 24 h, 93%; (e) H_2, 10% Pd-C, ethanol–HCl, rt, 3 h, 96%; (f) (1) benzoic acid derivative, diethyl cyanophosphonate, triethylamine, DMF, rt, 12–24 h, 46–82%; (2) LiOH–H_2O, 30% H_2O_2, THF/H_2O = 4:1 (v/v), 0 °C, 2.5 h then rt 3 h, 51–94%.

Healthcare), Benzamidine FF column (GE Healthcare), HisTrap HP column (GE Healthcare), HiTrap Q HP column (GE Healthcare), HiPrep 26/10 desalting column (GE Healthcare)). Apo PPARγ LBD crystals were soaked in ligand solution for two or three weeks prior to crystallography.

2.6. Diffraction data collection

The diffraction data for hPPARγ LBD complex with (***R***)-**7j** were collected on BL38B1 at SPring-8 (Harima, Japan) and were processed using HKL-2000.[25]

2.7. Structure analysis and refinement

The structure of hPPARα LBD complex with (***R***)-**7j** was solved by the molecular-replacement method with the program *CNS*[26] using the previously reported structures as probes. The correctly positioned molecules were refined with *CNS* and *O*.[27] The initial atomic model of (***R***)-**7j** was built using *MOE* (Ryoka Systems Inc.) and topology and parameter files for the refinement were generated by the *HIC-Up* server.[28]

The structure of hPPARγ LBD was solved by the molecular replacement method using Molrep. Apo PPARγ LBD structure (PDB code 1PRG) was used as a search model and refined with Refmac5. The crystallographic data and data collection statistics of all the crystals are provided in Table 1.

2.8. Adipogenesis assay

The adipogenesis assay was performed as previously described.[29] Mouse adipogenic fibroblast cells, 3T3-L1, were cultured in DMEM with 10% FBS. After the cells became confluent, they were pretreated with 1 μM dexamethasone (Dex), 0.5 mM 3-isobutyl-1-methylxanthine (IBMX), and 5 μg/mL insulin to initiate adipogenesis for 2 days. Various concentrations of ligands were added to the cells, and after 6 days, the cells were stained with Oil Red O. The degree of adipogenesis was quantitatively measured in terms of absorbance at OD550. The error bars are the standard deviations (SD).

2.9. Cell lines

A human scirrhous gastric cancer cell line, OCUM-2MD3[30] was cultured in DMEM/F12 (Ham) (1:1) (Invitrogen, Carlsbad, CA). A normal human fibroblast cell line, OUMS-24,[31] was cultured in DMEM (Nissui). All media were supplemented with 10% fetal bovine serum (Invitrogen), 100 μg/mL kanamycin (Meiji Seika, Tokyo, Japan) and 0.5 μg/mL Fungizone (Invitrogen).

2.10. Apoptosis assay

The apoptosis assay was performed as previously described.[32] Cells were inoculated into flat-bottomed 6-well plates, incubated for 24 h and then treated with test compound. Seventy-two hours later, 1 μg/mL Hoechst 33342 (Invitrogen) and 5 μg/mL propidium iodide (Sigma) were added to the medium and the cells were incubated in the dark for 20 min. All of the cells were collected on a glass slide and evaluated with a fluorescence microscope. Cells with fragmented or shrunken nuclei were counted as apoptotic cells.

3. Results and discussion

3.1. Structure–activity and structure–solubility relationships

In order to create phenylpropanoic acid-type PPARγ-selective agonists with improved aqueous solubility, we focused on the biphenyl derivative (***R***)-**7a** as a lead compound. The poor aqueous solubility of **3** might be attributed primarily to the presence of an adamantyl substituent at the hydrophobic tail part of the molecule, even though this substituent is one of the critical determinants for potent hPPARγ-selective agonistic activity. Although biphenyl derivative (***R***)-**7a** exhibited decreased activity compared with **3**, it still showed hPPARγ agonistic activity at sub-micromolar concentration (EC_{50} = 86 nM in our assay system).

We have previously reported biphenylcarboxylic acid-type hPPARδ partial agonists with improved aqueous solubility.[33] In that case, the improvement of solubility was attributed to two factors, that is, disruption of molecular planarity by the introduction of a substituent at the *ortho*-position of the attached benzene ring, and decreased hydrophobicity due to the introduction of a heteroaromatic ring. We also applied the same strategies in the present work, and the results are summarized in Table 1.

We evaluated the aqueous solubility of the compounds by calculating *C*log*P* values[34] and we also determined the retention times of the compounds in reversed-phase high-performance liquid chromatography (RP-HPLC). In the case of adamantyl derivative **3**, the *C*log*P* value is extremely high, more than 9, and the RP-HPLC retention time is about 30 min. These data clearly indicated that **3** is extremely hydrophobic, being even more hydrophobic than typical steroid drugs. However, in the case of the phenyl derivative (***R***)-**7a**, *C*log*P* is about 7.1, so that this compound is about 100 times more hydrophilic than **3**. In accordance with this, compound (***R***)-**7a** was eluted much faster than **3**, with a retention time of 7.9 min.

The *ortho*-substituted derivatives ((***R***)-**7b**, (***R***)-**7c**) exhibited comparable ((***R***)-**7b**) or somewhat increased ((***R***)-**7c**) hPPARγ agonistic activity. However, their aqueous solubility was not improved; indeed in the case of (***R***)-**7b**, it was decreased as compared to the non-substituted derivative (***R***)-**7a**. As expected, introduction of a small fluorine atom at the *meta* or *para* position ((***R***)-**7d**, (***R***)-**7e**) of the distal benzene ring did not significantly affect the in vitro biological activity or the aqueous solubility.

It is interesting to note that thiophen-2-yl phenyl derivative (***R***)-**7f** exhibited somewhat greater aqueous solubility with retention of the hPPARγ agonistic activity, as compared to the phenyl derivative (***R***)-**7a**. Although the thiophene ring, a well-known bioisostere of the benzene ring, is less hydrophobic than the benzene ring, the hydrophobicity of (***R***)-**7f** was increased. The reason for this is unclear. In any event, unsymmetrization of the biphenyl moiety of (***R***)-**7a** by the introduction of a substituent at the *ortho*-position of the benzene ring or by replacement of one of the benzene rings with an bioisostere was not very effective in this case. Therefore, we next tried to substitute a heterocyclic ring (pyridine, ((***R***)-**7g**–(***R***)-**7i**), pyrimidine ((***R***)-**7j**, (***R***)-**7l**), pyrazine ((***R***)-**7k**)) at the distal benzene ring. The results are included in Table 1. The position of the nitrogen atom of the monoazine is important for potent hPPARγ agonistic activity, that is, the hPPARγ agonistic activity decreased in the order of 2-pyridyl ((***R***)-**7g**) > 3-pyridyl ((***R***)-**7h**) > 4-pyridyl ((***R***)-**7i**), and pyrimidin-2-yl ((***R***)-**7j**) > pyradin-2-yl ((***R***)-**7h**) > pyrimidin-5-yl ((***R***)-**7i**). These results indicated that the distal nitrogen atom interacts unfavorably with the hPPARγ LBD, causing a considerable decrease of the activity.

As for aqueous solubility, the introduction of a pyridine ring instead of the benzene ring as the distal substituent improved the aqueous solubility by 10-fold, as judged from *C*log*P* (7.18 to 6.04 and 5.83). In accordance with this, (***R***)-**7g**–(***R***)-**7i** (retention times: 3.6, 2.3 and 1.8 min, respectively) were eluted much faster than the phenyl analogue (***R***)-**7a** (retention time: 7.9 min). These compounds exhibited similar ClogP values, whereas their retention times were somewhat different, that is, the compounds eluted faster in the order of (***R***)-**7i** (4-pyridyl) > (***R***)-**7h** (3-pyridyl) > (***R***)-**7g** (2-pyridyl). Thus, it appears that these two hydrophobic parameters do not necessarily correlate well.

Table 1
hPPARγ transactivation activities, *C*log*P* values and retention times (rt) on reversed-phase HPLC of the present series of derivatives

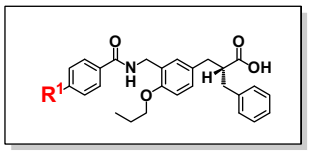

No.	R	EC_{50}[a] (nM) hPPARγ	Efficacy[b]	*C*log*P*[c]	rt[d] (min)	Aqueous solubility[f] (μg/mL)	No.	R	EC_{50}[a] (nM) hPPARγ	Efficacy[b]	*C*log*P*[c]	rt[d] (min)	Aqueous solubility[f] (μg/mL)
3		3.60	NT[e]	9.58	30.5 ± 0.02	<1.00							
7a		85.9	95.7	7.18	7.89 ± 0.01	<1.00	**7g**		186.1	113	6.04	3.57 ± 0.01	17.0
7b		73.8	72.7	7.38	9.71 ± 0.01	<1.00	**7h**		844	100	5.83	2.31 ± 0.01	69.5
7c		49.5	95.0	7.37	7.66 ± 0.01	<1.00	**7i**		1688	108	5.83	1.78 ± 0.01	34.1
7d	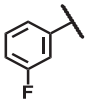	28.7	99.7	7.37	8.10 ± 0.01	<1.00	**7j**		34.6	65.0	5.12	4.25 ± 0.01	301
7e	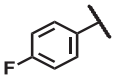	102.6	104	7.37	7.82 ± 0.02	<1.00	**7k**		713.9	58.2	5.12	3.845 ± 0.01	32.2
7f		65.2	76.0	7.37	7.42 ± 0.01	<1.00	**7l**		3095	82.7	4.91	3.23 ± 0.01	190

[a,b] EC_{50} values and % efficacy are given relative to the positive control, rosiglitazone for PPARγ.
[c] *C*Log*P* values were estimated with ChemDraw Ultra version 10.0.
[d] PegasilODS SP100 column (4.6 mm × 150 mm; flow rate of 1 mL/min; solvent, MeCN: 0.1% TFA = 3:1 v/v; detection at 254 nm or 296 nm).
[e] NT means not tested.
[f] Aqueous solubility in phosphate buffer (pH = 7.2–7.4).

In the case of (***R***)-**7j**–(***R***)-**7l,** the position of the nitrogen atom is also important for potency towards hPPARγ. The pyrimidin-2-yl derivative ((***R***)-**7j**) exhibited potent activity, comparable to that of the phenyl analog ((***R***)-**7a**). However, others, that is, the pyrazin-2-yl ((***R***)-**7k**) and pyrimidin-5-yl ((***R***)-**7l**) derivatives, exhibited decreased hPPARγ agonistic activity. These results indicated that *meta* position nitrogen atoms interact unfavorably with hPPARγ LBD, thereby decreasing the activity.

As for aqueous solubility, (***R***)-**7j**–(***R***)-**7l** exhibited about 100-fold increased aqueous solubility, as judged from *C*log*P* (from 7.18 for (***R***)-**7a** to 5.12, 5.12 and 4.91, respectively). In accordance with this, these diazines were eluted more quickly than the phenyl analogue (***R***)-**7a**. However, they were eluted more slowly than the pyridine derivatives (***R***)-**7g**–(***R***)-**7i**. These results indicate that introduction of hydrophilic aromatics, such as a pyridine ring or pyrimidine ring, is an effective strategy to improve the aqueous solubility of the present series of compounds.

We then assessed the exact thermodynamic solubility of these compounds. As expected, all the biphenyl derivatives ((***R***)-**7a**–(***R***)-**7f**) exhibited very poor aqueous solubility (<1 μg/mL), but the introduction of a nitrogen atom at the distal benzene ring improved the solubility to 17.0 μg/mL ((***R***)-**7g**) and 301 μg/mL ((***R***)-**7j**). The number of introduced nitrogen atoms was correlated with the thermodynamic solubility. We selected compound (***R***)-**7j** for further evaluation, based on its activity towards hPPARγ and good aqueous solubility. The intrinsic activity of (***R***)-**7j** suggests that it is a partial agonist, with the ability to activate hPPARγ to the extent of about 65% of the maximum activity observed with the full-agonist pioglitazone (**1**).

3.2. Partial-agonistic activity of (*R*)-7j

To characterize the hPPARγ partial-agonistic profile of (***R***)-**7j**, we compared the ability of **2** (an hPPARγ full-agonist), and (***R***)-**7j** to stimulate adipocyte differentiation of murine preadipocyte 3T3-L1 cells (Fig. 2). It is well known that PPARγ agonists promote the conversion of a variety of preadipocyte and stem cell lines into mature adipocytes.[35] Both compounds in the concentration range from 1 to 1000 nM stimulated adipocyte differentiation and induced triglyceride accumulation, as indicated by Oil Red O staining. Compound **2** exhibited dose-dependent adipocyte differentiation-promoting ability, providing the maximum absorption intensity (OD_{550} = 0.2 in these experiments). On the other hand, (***R***)-**7j** stimulated adipocyte differentiation at the lowest concentration of 1 nM, but dose-dependency was not maintained at high concentration and the absorption intensity was about 60% of the maximum at every concentration tested. These results indicate that (***R***)-**7j** is a hPPARγ partial-agonist.

3.3. Structural features of the complex of (*R*)-7j with hPPARγ ligand-binding domain (LBD)

To understand the structural basis for the activity of (***R***)-**7j**, we examined the three-dimensional structure of (***R***)-**7j** complexed

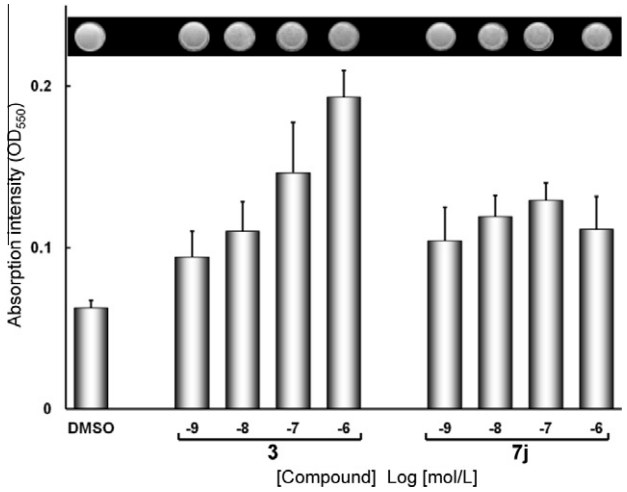

Figure 2. Adipogenesis-inducing activity of **3** and (***R***)-**7j**. After pretreatment with 1 μM Dex, 0.5 mM IBMX, and 5 μg/mL insulin, 3T3-L1 cells were incubated with the indicated concentrations of **3** and (***R***)-**7j**, respectively. Oil red O-stained cells are shown at the top and are quantified at the bottom by measurement of OD_{550} (±SD).

with the hPPARγ LBD by means of X-ray crystallographic analysis. The resulting three-dimensional structures of hPPARγ LBD–(***R***)-**7j** complex are illustrated in Figure 3A–G. The crystallographic data and refinement statistics are summarized in Table 2.

Like the reported structure of the hPPARγ LBD–**3** complex, hPPARγ LBD has a three-layered sandwich folded structure comprising mainly α-helices, and the overall interaction mode with the ligand is basically conserved.

The pyrimidin-2-yl derivative (***R***)-**7j** exhibited somewhat weaker hPPARγ agonistic activity than the adamantyl derivative **3**, and the X-ray crystallographic analysis of hPPARγ LBD–(***R***)-**7j** complex clearly revealed the reason for this difference. The pyrimidin-2-yl ring and adamantyl ring are hosted in the same binding pocket, that is, the large Y3 arm[36] cavity composed of the side chains of amino acid residues Leu255, Glu259, Ile262, Phe264, Arg280 and Ile281 (Fig. 3D and E). The planar pyrimidin-2-yl ring would interact less effectively with this large hydrophobic cavity, as compared to the three-dimensionally expanded hydrophobic adamantyl ring, especially as regards the hydrophobic interactions with Ile262, Phe264, and Ile 281, which are positioned on both sides of the pyrimidin-2-yl ring of (***R***)-**7j** (Fig. 3F and G).

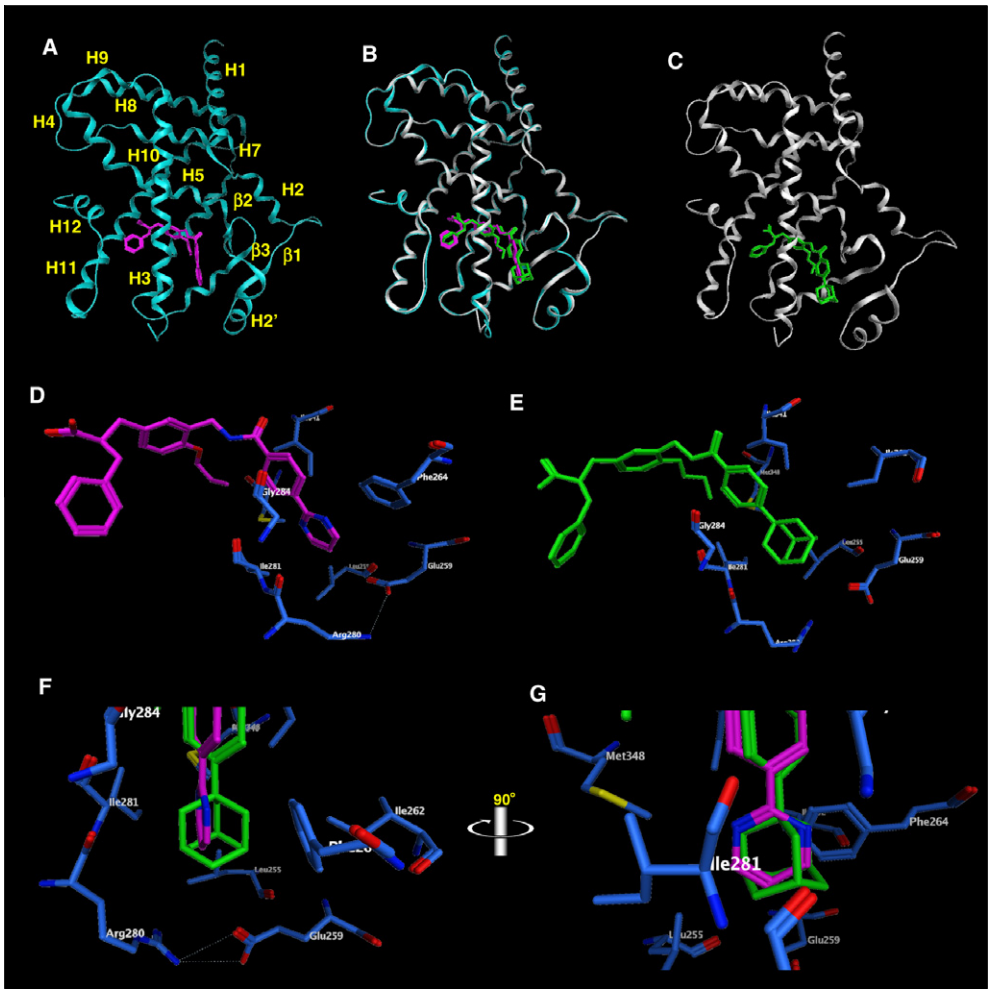

Figure 3. (A–G) Crystal structures of hPPARγ LBD–**3** complex (PDB: 2ZNO) and hPPARγ LBD–(***R***)-**7j** complex (PDB: 3VSO). (A) Whole structure of hPPARγLBD–(***R***)-**7j** complex. Protein is represented as a blue ribbon model and (***R***)-**7j** is depicted as a magenta cylinder model. The numbering of the second structure is also depicted. The nomenclature of the helices is based on the RXR-α crystal structure. (B) The superimposed structures of **3** and (***R***)-**7j** complexed with hPPARγ LBD. (C) Whole structure of hPPARγ LBD–**3** complex. Protein is represented as a white ribbon model and **3** is depicted as a green cylinder model. (D) Zoomed view of the binding mode of the hydrophobic tail part of **3** in the Y3 arm. The side chains of amino acids of the Y3 arm are depicted as blue cylinder models. (E) Zoomed view of the binding mode of the hydrophobic tail part of (***R***)-**7j** in the Y3 arm. (F) Zoomed view of the alinement of the hydrophobic tail part of **3** and (***R***)-**7j**. (G) image F rotated by 90°.

Table 2
Crystallographic data and refinement statistics

Crystal	PPARg-7j
Data collection	
Space group	*C*2
Unit cell constants	
a (Å)	93.35
b (Å)	61.71
c (Å)	118.98
β (°)	102.79
Wavelength (Å)	1
Resolution[a] (Å)	50.0–1.97
(Highest shell)	2.04–1.97
Measured reflections	172342(16510)
Unique reflections	46474(4586)
Completeness	99.2(99.7)
$I/\sigma(I)$	17.2(3.7)
Redundancy	3.7(3.6)
R_{merge}[b]	4.2(40.1)
Refinement	
Resolution (Å)	30.0–2.0
R_{work}[c]/R_{free}[d] (%)	21.9/25.7
Number of atoms	
Protein	4184
Water	117
Ligand	38
Average B-factor (Å²)	
Protein	41.3
Water	36.7
Ligand	57
r.m.s.d.	
Bond Lengths (Å)	0.007
Angles (°)	1.0
PDB code	3VSO

[a] Values in parentheses indicate statistics for the highest resolution shells.
[b] $R_{merge} = \Sigma_{hkl}\Sigma_i|I_i(hkl) - \langle I(hkl)\rangle|/\Sigma_{hkl}\Sigma_i I_i(hkl)$, where $\langle I(hkl)\rangle$ is the mean $I(hkl)$ over symmetry-equivalent reflections.
[c] $R_{work} = \Sigma_{hkl}|F_{obs} - F_{calc}|/\Sigma_{hkl}|F_{obs}|$, where F_{obs} and F_{calc} are the observed and calculated structure factors, respectively.
[d] R_{free} was calculated using 5% of the total reflections, which were chosen randomly and omitted from the refinement.

It is interesting to note Glu259 and Arg280 show a hydrogen bonding interaction to form a 'salt bridge'[37] that determines the depth of the Y3 arm. The rank order of the decrease in hPPARγ agonistic activity of 4-pyridyl ((***R***)-**7i**) > 3-pyridyl ((***R***)-**7h**) > 2-pyridyl ((***R***)-**7g**) derivatives might be attributed to unfavorable interaction between the nitrogen atom of the distal heteroaromatic ring and the anionic side chain of Glu259.

3.4. Structural basis of the partial agonism of (*R*)-7j towards hPPARγ

The qualitative characteristics of corepressor dissociation and coactivator recruitment are reported to be regulated differentially by the three-dimensional structure around the C-terminal H12 helix and the surrounding helixes of the nuclear receptor.[38] In the case of the binding of a full agonist, such as rosiglitazone, the H12 helix forms a part of the coactivator-binding surface, along with the H3 helix and H5 helix.[39] In this case, the positions and directions of the side chains of two distinct hydrophilic amino acids, Lys301 (in H3 helix) and Glu471 (in H12 helix), are reported to be critically important, because these amino acids clamp the LXXLL motif (L, leucine; X, any amino acid) of the coactivator, and dock it appropriately to express full-agonistic activity.[39] Therefore, we first compared the three-dimensional structures of two PPARγ full agonists, rosiglitazone and farglitazar,[40] complexed with hPPARγ LBD[41] (Fig. 4A–F).

The main frameworks of hPPARγ LBD complexed with rosiglitazone and farglitazar are depicted in Figure 4A, B, and a superposition of these two complexes is shown in Figure 4C. The overall folds are well matched in these two complexes, and the positions and the directions of the side chains of Lys301 and Glu471 overlap well in these structures. The root mean square deviations (RSMDs) of these two amino acid residues are 0.71 and 0.44 Å, respectively (Fig. 4E, F).[42] These results indicate that the two hPPARγ full agonists will be able to recruit coactivator complexes with almost the same efficacy, eliciting full agonistic activity.

On the other hand, the overall structures of hPPARγ LBD complexed with hPPARγ partial agonists, including **(*R*)-7j**, are somewhat different. The frameworks of hPPARγ LBD complexed with several representative hPPARγ partial agonists ((***R***)-**7j**, LT127,[43] phenoxyacetic acid derivative,[44] GW-0072,[45] pyrazole derivative,[46] and GQ-16[47]) are depicted in Figure 5A–F, and a superposition of the six complexes is shown in Figure 5G. The folds of the upper half of the hPPARγ LBD, composed of the H1, H2, H4, H5, H8 and H9 helixes, are well matched in these complexes. However, the folds of the lower half of the hPPARγ LBD, composed of H2′, H3, H6, H10–H12 helixes and β1–β3 sheets, are somewhat different. The position of Lys301 in the H3 helix varies somewhat (RMSD = 1.10 Å, as compared to 0.71 Å for full agonists) in these structures. However, the side chain of Glu471 in the H12 helix faces in various directions in these complexes, and the RSMD is much larger (1.89 Å as compared to 0.44 Å for full agonists). These substantial differences in structure might be one of the driving forces behind the partial agonistic activity of these compounds, including (***R***)-**7j**.

To better understand the key differences in the binding of hPPARγ full agonists and hPPARγ partial agonists, we focused on the binding mode of these agonists to Tyr473 in the H12 helix. As already reported, Tyr473 is believed to play a critical role in the full agonist-mediated stabilization of the LBD of hPPARγ (Fig. 6A–C). In the case of the full agonist rosiglitazone, the side chain phenol oxygen of Tyr473 forms a tight hydrogen bond with the nitrogen atom of the thiazolidine-2,4-dione ring. Furthermore, the side chain phenol oxygen of Tyr473 has a hydrogen bonding interaction with the carbonyl oxygen atom of the thiazolidine-2,4-dione ring. These hydrogen bonding interactions tightly fix Tyr473 in the H12 helix, forming a section of the tranccriptional coactivator-binding surface of the PPARγ LBD Figure 6A.

In the case of the partial agonist *N*-[1-(4-fluorophenyl)-3-(2-thenyl)-1*H*-pyrazole-5-yl]-3,5-bis-(trifluoromethyl)benzenesulfonamide (PDB: 2GOH), the 4-fluorophenyl ring is located close to the H12 helix, but it has no hydrophobic or hydrogen bonding interaction with this helix (Fig. 6C). Therefore, there is no significant ligand-mediated interaction to fix Tyr473 in the H12 helix. The absence of interaction (or the presence of weak interaction) with Tyr473 in the H12 helix could provide the structural basis for the partial agonist functionality of not only this compound, but also the other neutral-and carboxylic acid-type hPPARγ partial agonists shown in Figures 5B–F 6B.

In the case of α-benzylphenylpropanoic acid **(*R*)-7j**, the acidic carboxylic acid moiety hydrogen bonds with the side chain phenol oxygen of Tyr473. However, the distance between these two functionalities is longer than that in the case of hPPARγ LBD complexed with the thiazolidine-2,4-dione-type hPPARγ full agonist, rosiglitazone. Furthermore, there is only a single hydrogen bonding interaction between the acidic moiety of **(*R*)-7j** and Tyr473 in the H12 helix. Considering these two factors, Tyr473 in the H12 helix is thought to be fixed less effectively when **(*R*)-7j** is bound to hPPARγ-LBD, resulting in partial agonistic activity Figure 6B.

3.5. Preliminal apoptotic effect of (*R*)-7j on scirrhous gastric cancer cell line

In order to investigate the potential of hPPARγ partial agonist (***R***)-**7j** as an anti-scirrhous gastric cancer agent, we preliminally compared the apoptosis-inducing effect of (***R***)-**7j** and **3**, together

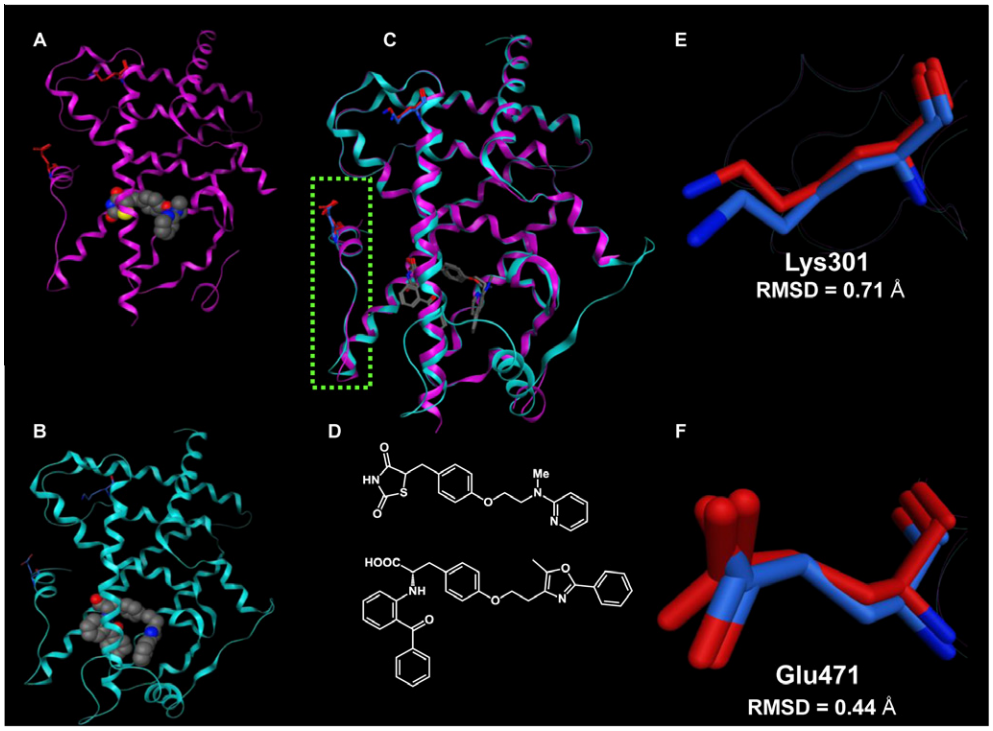

Figure 4. (A, B) Crystal structures of hPPARγ LBD–rosiglitazone (full agonist) complex (PDB: 2PRG) and hPPARγ LBD–farglitazar (full agonist) complex (PDB: 1FM9). (C) The superimposed structures of hPPARγ LBD–rosiglitazone complex and hPPARγ LBD–farglitazar. Both ligands are depicted as cylinder models, and Lys301 and Glu473 are highlighted as cylinder models in magenta (rosiglitazone complex) and cyan (farglitazar complex). The N-terminal AF2 region (H12 helix) is highlighted as a light green dotted box. (D) Chemical structures of rosiglitazone and farglitazar. (E) Zoomed view of the superimposed Lys301 of hPPARγ LBD–rosiglitazone complex and hPPARγ LBD–farglitazar complex. Lys301 is highlighted as a cylinder model in magenta (rosiglitazone complex) or blue (farglitazar). (F) Zoomed view of the superimposed Glu473 of hPPARγ LBD–rosiglitazone complex and hPPARγ LBD–farglitazar complex. Glu473 is highlighted as a cylinder model in magenta (rosiglitazone complex) or blue (farglitazar).

with the hPPARγ full agonist troglitazone, on human scirrhous gastric cancer cell line OCUM-2MD3. Troglitazone was used as a positive control, based on reports that it suppresses the growth of gastric cancer cell lines, such as MKV45 cells,[48] SNU-216 and SNU-668 cells.[49]

OCUM-2MD3 cells and OUMS-24 (a normal human fibroblast cell line) cells were incubated for 24 h and then treated with the indicated concentrations of test compounds. After 72 h, Hoechst 33342 and propidium iodide were added to the medium, and the cells were incubated in the dark for 20 min. All the cells were then collected on a glass slide, and evaluated under a fluorescence microscope. Cells with fragmented and/or shrunken nuclei were counted as apoptotic cells. The results, expressed as % increase of apoptotic cells versus the DMSO control, are illustrated in Figure 7.

Troglitazone (hPPARγ full agonist) dose-dependently enhanced apoptosis in the concentration range of 1–100 μM. Thus, troglitazone induces apoptosis of human scirrhous gastric cancer cell line OCUM-2MD3, as well as the other gastric cancer cell lines, MKV45, SNU-216 and SNU-668,[48,49] while it exhibited little effect on normal cells. The finding that troglitazone selectively induced apoptosis of human scirrhous gastric cancer cells is important, even though the reason is unknown. One possibility is that different amounts of PPARγ may be expressed in the cell lines.

The hPPARγ full agonist **3** also dose-dependently enhanced apoptosis in the concentration range of 1–100 μM, and it was more potent than troglitazone (10 μM **3** effectively induced apoptosis of OCUM-2MD3 cells). However, 100 μM **3** induced apoptosis of both OCUM-2MD3 and OCUM-24 cell lines. Therefore, **3** may show poorer selectivity for human scirrhous gastric cancer cells, as compared to troglitazone.

Finally, we found that hPPARγ partial agonist (***R***)-**7j** also effectively induced apoptosis of OCUM-2MD3 cells. Treatment of (***R***)-**7j** also dose-dependently enhanced apoptosis in the concentration range of 1–100 μM. The potency was equal to or somewhat greater than that of the hPPARγ full-agonist troglitazone (based on the activity at 10 μM). Furthermore, (***R***)-**7j** shows high selectivity for cancer cells, comparable to that of troglitazone. These results indicated that partial activation of PPARγ might sufficient to induce apoptosis of human scirrhous gastric cancer cells.

In conclusion, we have created the novel α-benzyl phenylpropanoic acid-type hPPARγ partial agonist (***R***)-**7j**, which shows increased aqueous solubility as a result of replacement of the adamantyl group of **3** with a pyrimidin-2-yl group. It also selectively induced apoptosis of OCUM-2MD3 human scirrhous gastric cancer cells. In vivo pharmacological evaluation of **7j** as anti-scirrhous gastric cancer agent is under way.

4. Experimental section

4.1. Chemistry: general methods

Melting points were determined with a Yanagimoto hot-stage melting point apparatus and are uncorrected. ^{1}H NMR and ^{13}C NMR spectra were recorded on a Varian VNMRS-400 (400 MHz) SC-NMR spectrometer. Proton chemical shifts were referenced to TMS as an internal standard. FAB-MS was carried out with a VG70-SE. Chiral HPLC analyses were performed on an analytical column (CHIRALPAK IA column (4.6 × 150 mm; detection at 254 nm). HPLC analyses were performed on an analytical column (PegasilODS SP100 column (4.6 × 150 mm; flow rate of 1 mL/min; solvent, MeCN/0.1% TFA = 3:1 v/v; detection at 254–296 nm). All optical rotation data was recorded at 25 °C on a Jasco P-2000 polarimeter with a 50 mm cell (concentration reported as g/100 mL).

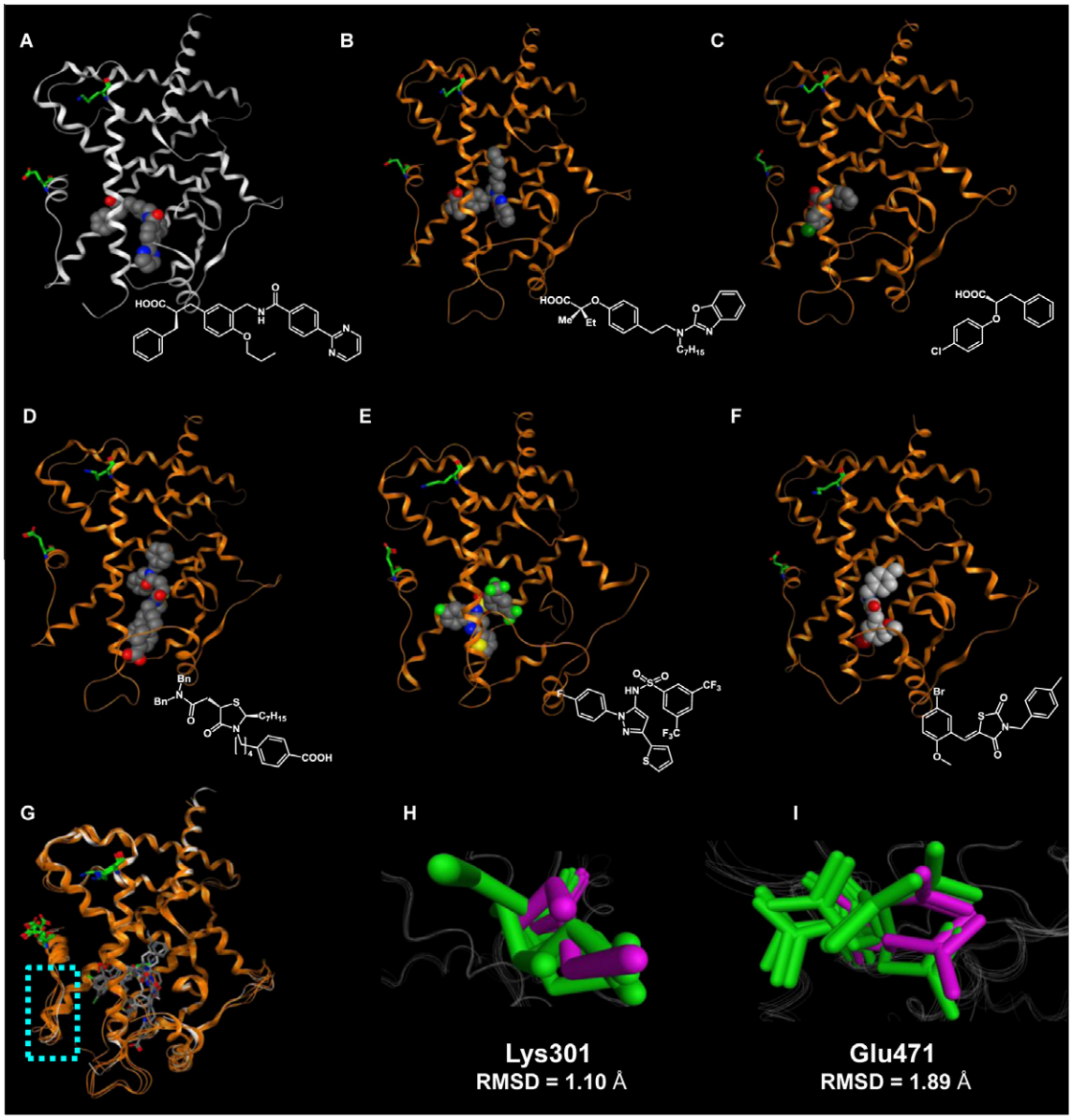

Figure 5. (A–F) Crystal structures of hPPARγ LBD–partial agonist complexes. (A) Crystal structure of hPPARγ LBD–**7j** complex (PDB: 3VSO). (B) Crystal structure of hPPARγ LBD–LT127 complex (PDB: 2I4Z). (C) Crystal structure of hPPARγ LBD–(2*S*)-2-(4-chlorophenoxy)-3-phenylpropanoic acid complex (PDB: 3CDP). (D) Crystal structure of hPPARγ LBD–GW-0072 complex (PDB: 4PRG). (E) Crystal structure of hPPARγ LBD–*N*-[1-(4-fluorophenyl)-3-(2-thenyl)-1*H*-pyrazole-5-yl]-3,5-bis(trifluoromethyl)benzenesulfonamide complex (PDB: 2GOH). (F) Crystal structure of hPPARγ LBD–GQ-16 complex (PDB: 3T03). (G) The superimposed structures of hPPARγ LBD–partial agonist complexes. All ligands are depicted as cylinder models, and Lys301 and Glu473 are highlighted as green cylinder models. The N-terminal AF2 region (H12 helix) is highlighted as a light green dotted box. (H) Zoomed view of the superimposed Lys301 of hPPARγ LBD–partial agonist complexes. All Lys301 residus are highlighted as a green cylinder model. (I) Zoomed view of the superimposed Glu473 of hPPARγ LBD–partial agonist complexes. All Glu473 residues are also highlighted as a green cylinder model.

4.2. (*R*)-2-(3-([1,1′-Biphenyl]-4-ylcarboxamidomethyl)-4-propoxybenzyl)-3-phenylpropanoic acid ((*R*)-7a)

A mixture of 5-((*R*)-2-benzyl-3-((*S*)-4-benzyl-2-oxo-oxazolidin-3-yl)-3-oxopropyl)-2-propoxy-benzaldehyde (**6**) (250 mg, 0.51 mmol), 4-phenylbenzamide (300 mg, 1.54 mmol), triethylsilane (0.25 mL, 1.54 mmol), trifluoroacetic acid (0.12 mL, 1.54 mmol) and 40 mL of dehydrated toluene was refluxed for 48 h under an argon atmosphere. The reaction mixture was poured into water, and the whole was extracted with ethyl acetate. The extract was washed with brine, dried over anhydrous magnesium sulfate and concentrated. The residue was purified by silica gel column chromatography (eluant; *n*-hexane/ethyl acetate = 1:1 v/v) to afford 162 mg (47%) of the intermediate derivative as a pale yellow solid. ^{1}H NMR (400 MHz, $CDCl_3$) δ 7.74 (d, J = 8.4 Hz, 2H), 7.58 (t, J = 8.6 Hz, 4H), 7.45 (t, J = 7.4 Hz, 2H), 7.37 (t, J = 7.4 Hz, 1H), 7.29–7.15 (m, 10H), 6.88–6.85 (m, 2H), 6.81 (d, J = 8.4 Hz, 1H), 6.61 (t, J = 5.2 Hz, 1H), 4.69 (dd, J = 14.4, 5.6 Hz, 1H), 4.64–4.55 (m, 2H), 4.41–4.35 (m, 1H), 4.00–3.93 (m, 2H), 3.90 (dd, J = 8.8, 2.4 Hz, 1H), 3.74 (t, J = 8.2 Hz, 1H), 3.08 (dd, J = 13.4, 9.0 Hz, 1H), 2.98 (dd, J = 13.4, 9.0 Hz, 1H), 2.91–2.78 (m, 3H), 2.51 (dd, J = 13.4, 8.6 Hz, 1H), 1.87–1.78 (m, 2H), 1.04 (t, J = 7.4 Hz, 3H); MS (FAB) 667 $(M+H)^+$.

This intermediate (157 mg, 0.24 mmol) was dissolved in 16 mL of tetrahydrofuran and 4 mL of water under an argon atmosphere with ice-cooling. To this solution was added 30% aqueous hydrogen peroxide (0.27 mL, 2.40 mmol). Then a solution of lithium hydroxide monohydrate (40 mg, 0.96 mmol) in water (1 mL) was added, and the mixture was stirred for 3.5 h at 0 °C. An aqueous

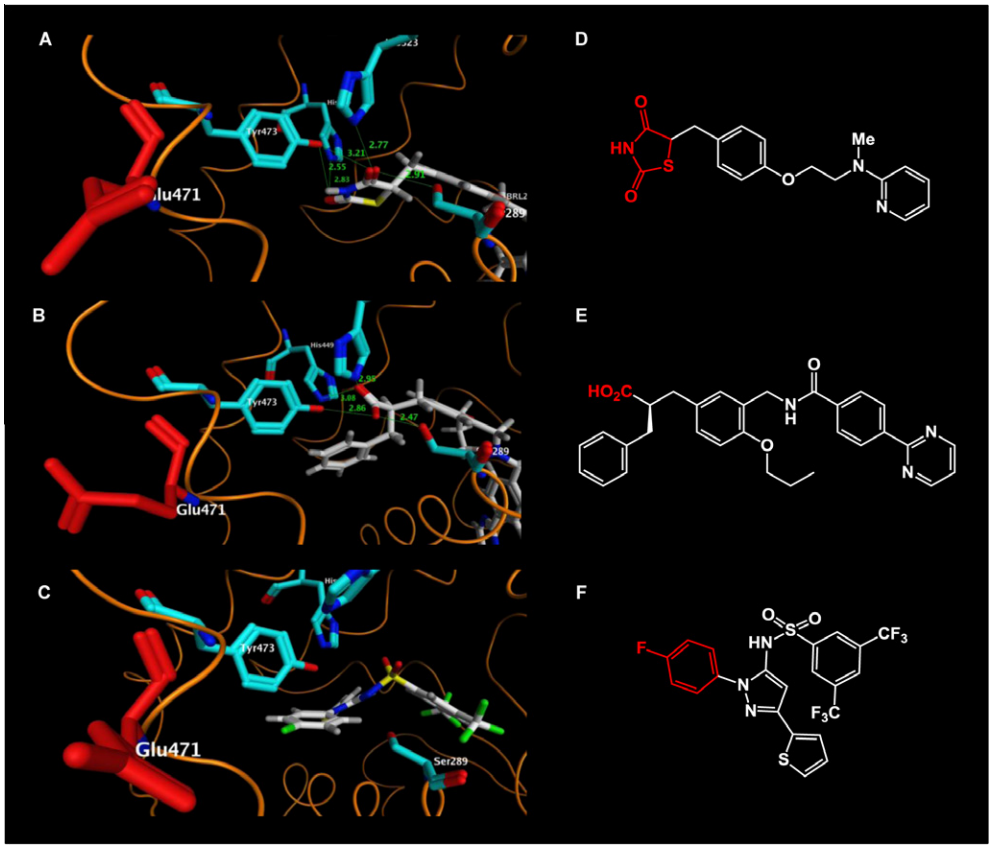

Figure 6. (A–C) Zoomed views of the binding mode of the AF2 region (H12 helix) of hPPARγ LBD–rosiglitazone. (A) Zoomed view of hPPARγ LBD–rosiglitazone (full agonist) complex. (B) Zoomed view of hPPARγ LBD–**7j** (partial agonist) complex. (C) Zoomed view of hPPARγ LBD–*N*-[1-(4-fluorophenyl)-3-(2-thenyl)-1*H*-pyrazole-5-yl]-3,5-bis(trifluoromethyl)benzenesulfonamide (partial agonist) complex.

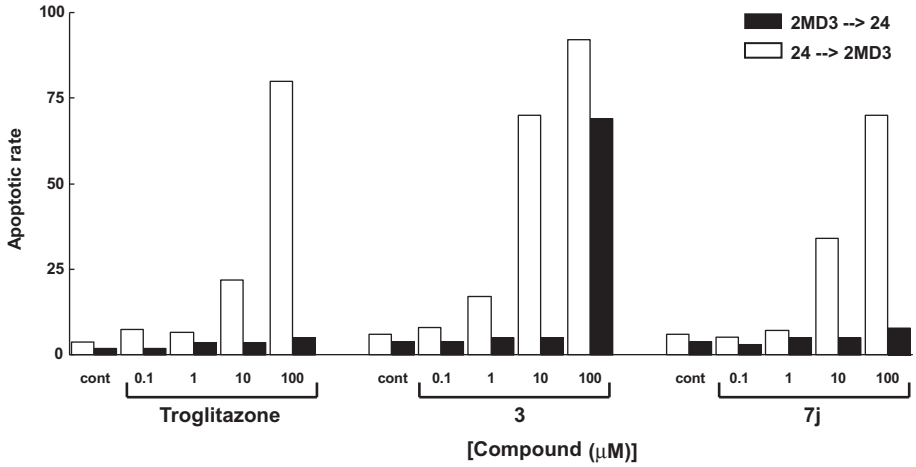

Figure 7. Apoptosis-inducing activity of troglitazone, **3** and (***R***)-**7j** on OCUM-2MD3 and OUMS-24 cells.

solution of sodium sulfite (1.00 g/6 mL) was further added and stirring was continued for 15 min. The reaction mixture was acidified with 10% HCl, and then extracted with ethyl acetate. The extract was washed with brine, dried over anhydrous magnesium sulfate and concentrated. The residue was purified by silica gel column chromatography (eluant; *n*-hexane/ethyl acetate = 1:1 v/v) to afford 100 mg (82%) of the title compound as a white amorphous solid. ^{1}H NMR (400 MHz, $CDCl_3$) δ 7.80 (d, J = 8.4 Hz, 2H), 7.63–7.57 (m, 4H), 7.45 (t, J = 7.4 Hz, 2H), 7.37 (t, J = 7.4 Hz, 1H), 7.27–7.23 (m, 2H), 7.04 (dd, J = 8.4, 2.4 Hz, 1H), 6.81 (t, J = 5.8 Hz, 1H), 6.77 (d, J = 8.0 Hz, 1H), 4.65–4.55 (m, 2H), 3.95 (t, J = 6.4 Hz, 2H), 3.02–2.86 (m, 3H), 2.80–2.73 (m, 2H), 1.88–1.79 (m, 2H), 1.05 (t, J = 7.4 Hz, 3H); ^{13}C NMR (300 MHz, $CDCl_3$) δ 178.85, 167.07, 155.74, 144.11, 140.01, 138.92, 133.25, 130.90, 130.46, 129.18, 128.91, 128.87, 128.42, 127.92, 127.44, 127.16, 126.39, 125.94, 111.12, 69.50, 49.42, 40.31, 37.80, 36.92, 22.74, 10.74; MS (FAB) 508 $(M+H)^+$; calcd for $C_{33}H_{34}NO_4$ 508.2487, found 508.2503; $[\alpha]_D$ −8.7° (c 0.25, CH_3CN). The enantiomeric excess (ee) of this compound was determined to be >98% by chiral HPLC, using a 4.6 × 250 mm CHIRALPAK IA column (Diacel Chemical Industries, Ltd), eluting at a flow rate of 0.5 mL/min with 2-propanol/*n*-hexane/TFA (1:2:0.03 v/v/v): retention time 17.4 min (the *S* enantio-

mer has a retention time of 15.4 min); HPLC purity was estimated to be 99.8% by means of reversed-phase HPLC, using a Pegasil ODS sp100 column (4.6 × 250 mm, Senshu Chemical, Japan) fitted on a Shimadzu HPLC system, with CH_3CN/0.1% TFA = 3:1 v/v as the eluant and detection at 254 nm.

4.3. (*R*)-2-Benzyl-3-(3-((2′-methyl-[1,1′-biphenyl]-4-ylcarboxamido)methyl)-4-propoxy-phenyl)propanoic acid ((*R*)-7b)

This compound was prepared by means of a procedure similar to that used for **7a**. ^{1}H NMR (400 MHz, $CDCl_3$) δ 7.78 (d, J = 8.4 Hz, 2H), 7.35 (d, J = 8.4 Hz, 2H), 7.28–7.22 (m, 5H), 7.20–7.17 (m, 5H), 7.04 (dd, J = 8.4, 2.2 Hz, 1H), 6.81–6.76 (m, 2H), 4.65–4.56 (m, 2H), 3.96 (t, J = 6.4 Hz, 2H), 3.02–2.87 (m, 3H), 2.82–2.73 (m, 2H), 2.24 (s, 3H), 1.88–1.80 (m, 2H), 1.06 (t, J = 7.4 Hz, 3H); ^{13}C NMR (300 MHz, $CDCl_3$) δ 178.82, 167.16, 155.77, 145.13, 140.85, 138.87, 135.21, 133.01, 130.82, 130.53, 130.45, 129.57, 129.38, 129.20, 128.92, 128.45, 127.75, 126.76, 126.44, 125.99, 125.88, 111.12, 69.51, 49.35, 40.31, 37.75, 36.94, 22.75, 20.40, 10.77; MS (FAB) 522 $(M+H)^+$; calcd for $C_{34}H_{36}NO_4$ 522.2644, found 522.2660; $[\alpha]_D$ −9.3° (c 0.25, CH_3CN). The enantiomeric excess (ee) of this compound was determined to be 97% by chiral HPLC using a 4.6 × 250 mm CHIRALPAK IA column (Diacel Chemical Industries, Ltd), eluting at a flow rate of 0.5 mL/min with 2-propanol/*n*-hexane/TFA (1:2:0.03 v/v/v): retention time 14.5 min (the *S* enantiomer has a retention time of 13.2 min); HPLC purity was estimated to be 99.4% by means of reversed-phase HPLC, using a Pegasil ODS sp100 column (4.6 × 250 mm, Senshu Chemical, Japan) fitted on a Shimadzu HPLC system, with CH_3CN/0.1% TFA = 3:1 v/v as the eluant and detection at 254 nm.

4.4. (*R*)-2-Benzyl-3-(3-((2′-fluoro-[1,1′-biphenyl]-4-ylcarboxamido)methyl)-4-propoxy-phenyl)propanoic acid ((*R*)-7c)

This compound was prepared by means of a procedure similar to that used for **7a**.

^{1}H NMR (400 MHz, $CDCl_3$) δ 7.80 (d, J = 8.4 Hz, 2H), 7.59 (dd, J = 8.4, 1.6 Hz, 2H), 7.43 (dt, J = 7.6, 1.8 Hz, 1H), 7.37–7.32 (m, 1H), 7.28–7.14 (m, 8H), 6.80–6.76 (m, 2H), 4.65–4.56 (m, 2H), 3.95 (t, J = 6.6 Hz, 2H), 3.01–2.87 (m, 3H), 2.82–2.73 (m, 2H), 1.88–1.79 (m, 2H), 1.06 (t, J = 7.4 Hz, 3H); ^{13}C NMR (300 MHz, $CDCl_3$) δ 178.97, 166.96, 161.33, 158.04, 155.76, 138.86, 138.82, 138.81, 133.67, 130.82, 130.65, 130.61, 130.46, 129.67, 129.57, 129.21, 129.16, 129.12, 128.92, 128.45, 128.09, 127.91, 127.07, 126.43, 125.92, 124.52, 124.47, 116.37, 116.07, 111.12, 69.50, 49.37, 40.32, 37.77, 36.92, 22.75, 10.76; MS (FAB) 526 $(M+H)^+$; calcd for $C_{33}H_{33}FNO_4$ 526.2394, found 526.2399; $[\alpha]_D$ −8.5° (c 0.25, CH_3CN). The enantiomeric excess (ee) of this compound was determined to be 98% by chiral HPLC using a 4.6 × 250 mm CHIRALPAK IA column (Diacel Chemical Industries, Ltd), eluting at a flow rate of 0.5 mL/min with 2-propanol/*n*-hexane/TFA (1:2:0.03 v/v/v): retention time 15.7 min (the *S* enantiomer has a retention time of 14.6 min); HPLC purity was estimated to be 99.6% by means of reversed-phase HPLC, using a Pegasil ODS sp100 column (4.6 × 250 mm, Senshu Chemical, Japan) fitted on a Shimadzu HPLC system, with CH_3CN/0.1% TFA = 3:1 v/v as the eluant and detection at 254 nm.

4.5. (*R*)-2-Benzyl-3-(3-((4′-fluoro-[1,1′-biphenyl]-4-ylcarboxamido)methyl)-4-propoxy-phenyl)propanoic acid ((*R*)-7e)

This compound was prepared by means of a procedure similar to that used for **7a**.

^{1}H NMR (400 MHz, $CDCl_3$) δ 7.80 (d, J = 8.0 Hz, 2H), 7.57–7.52 (m, 4H), 7.27–7.23 (m, 2H), 7.20–7.11 (m, 6H), 7.04 (dd, J = 8.2, 2.2 Hz, 1H), 6.80–6.76 (m, 2H), 4.65–4.56 (m, 2H), 3.95 (t, J = 6.4 Hz, 2H), 3.01–2.87 (m, 3H), 2.81–2.73 (m, 2H), 1.88–1.79 (m, 2H), 1.05 (t, J = 7.4 Hz, 3H); ^{13}C NMR (300 MHz, $CDCl_3$) δ 179.13, 166.92, 164.42, 161.15, 155.57, 143.07, 138.82, 136.15, 133.27, 130.81, 130.45, 129.20, 128.90, 128.84, 128.74, 128.45, 127.52, 127.01, 126.44, 125.91, 115.95, 115.67, 111.12, 69.50, 49.35, 40.31, 37.73, 36.89, 22.74, 10.77; ^{13}C NMR (300 MHz, $CDCl_3$) δ 179.13, 166.92, 164.42, 161.15, 155.57, 143.07, 138.82, 136.15, 133.27, 130.81, 130.45, 129.20, 128.90, 128.84, 128.74, 128.45, 127.52, 127.01, 126.44, 125.91, 115.95, 115.67, 111.12, 69.50, 49.35, 40.31, 37.73, 36.89, 22.74, 10.77;MS (FAB) 526 $(M+H)^+$; calcd for $C_{33}H_{33}FNO_4$ 526.2394, found 526.2399; $[\alpha]_D$ −9.4° (c 0.25, CH_3CN). The enantiomeric excess (ee) of this compound was determined to be 97% by chiral HPLC using a 4.6 × 250 mm CHIRALPAK IA column (Diacel Chemical Industries, Ltd), eluting at a flow rate of 0.5 mL/min with 2-propanol/*n*-hexane/TFA (1:2:0.03 v/v/v): retention time 19.8 min (the *S* enantiomer has a retention time of 17.4 min); HPLC purity was estimated to be 99.9% by means of reversed-phase HPLC, using a Pegasil ODS sp100 column (4.6 × 250 mm, Senshu Chemical, Japan) fitted on a Shimadzu HPLC system, with CH_3CN/0.1% TFA = 3:1 v/v as the eluant and detection at 254 nm.

4.6. 5-((*R*)-2-Benzyl-3-((*S*)-4-benzyl-2-oxooxazolidin-3-yl)-3-oxopropyl)-2-propoxybenz-aldehyde oxime (8)

A mixture of **6** (3.31 g, 6.82 mmol), hydroxylamine hydrochloride (568 mg, 8.18 mmol), dehydrated pyridine (0.82 mL, 10.23 mmol) and 40 mL of ethanol was stirred overnight at room temperature. Excess ethanol was evaporated, and the residue was diluted with ethyl acetate, then washed with 1 mol/L HCl, a saturated aqueous solution of sodium hydrocarbonate and brine. The organic layer was separated, dried over anhydrous magnesium sulfate and concentrated to afford 3.18 g of the title compound as a colorless oil, which was used in the next step without further purification. ^{1}H NMR (400 MHz, $CDCl_3$) δ 8.50 (s, 1H), 7.65 (d, J = 1.6 Hz, 1H), 7.28–7.15 (m, 9H), 7.00 (dd, J = 7.6, 2.0 Hz, 2H), 6.81 (d, J = 8.4 Hz, 1H), 4.59–4.52 (m, 1H), 4.45–4.41 (m, 1H), 3.95–3.86 (m, 3H), 3.79 (t, J = 8.4 Hz, 1H), 3.08 (dd, J = 13.4. 8.2 Hz, 1H), 3.05–2.96 (m, 2H), 2.82 (dd, J = 13.4, 6.2 Hz, 1H), 2.78 (dd, J = 13.6, 6.4 Hz, 1H), 2.49 (dd, J = 13.2, 9.2 Hz, 1H), 1.84–1.75 (m, 2H), 1.02 (t, J = 7.4 Hz, 3H); MS (FAB) 501 $(M+H)^+$.

4.7. (*S*)-3-((*R*)-2-(3-(Aminomethyl)-4-propoxybenzyl)-3-phenylpropanoyl)-4-benzyl-oxazolidin-2-one hydrochloride (9)

A mixture of **8** (3.18 g, 6.35 mmol), 10% palladium on carbon (1.60 g), concentrated HCl (8 mL) and 50 mL of ethanol was subjected to catalytic hydrogenation at an initial hydrogen pressure of 400–500 kPa. After completion of the reaction, the catalyst was removed by filtration and the filtrate was concentrated to afford 3.30 g of the title compound as a pale yellow solid, which was used in the next step without further purification. MS (FAB) 487 $(M+H)^+$.

4.8. (*R*)-2-Benzyl-3-(4-propoxy-3-((4-(pyridin-2-yl)benzamido)methyl)phenyl)propanoic acid ((*R*)-7g)

Under an argon atmosphere, diethyl cyanophosphonate (DEPC) (0.09 mL, 0.61 mmol) and triethylamine (0.18 mL, 1.30 mmol) were added to a solution of compound **9** (246 mg, 0.47 mmol) and 4-(2-pyridyl)benzoic acid (94 mg, 0.47 mmol) in dehydrated *N*,*N*-dimethylformamide (10 mL) at 0 °C. The reaction mixture

was left to stand overnight, then poured into a saturated aqueous solution of sodium hydrocarbonate, and the whole was extracted with ethyl acetate. The extract was washed with brine, dried over anhydrous magnesium sulfate and concentrated. The residue was purified by silica gel column chromatography (eluant; *n*-hexane/ethyl acetate = 1:2 v/v) to afford 170 mg (54%) of the intermediate compound as a colorless oil. ^{1}H NMR (400 MHz, $CDCl_3$) δ 8.71 (d, J = 5.6 Hz, 1H), 8.00 (d, J = 8.4 Hz, 2H), 7.80–7.73 (m, 4H), 7.30–7.15 (m, 11H), 6.90–6.87 (m, 2H), 6.82 (d, J = 8.4 Hz, 1H), 6.66 (t, J = 5.4 Hz, 1H), 4.69 (dd, J = 14.6, 5.8 Hz, 1H), 4.64–4.55 (m, 2H), 4.41–4.35 (m, 1H), 4.00–3.92 (m, 2H), 3.90 (dd, J = 8.8, 2.4 Hz, 1H), 3.74 (t, J = 8.4 Hz, 1H), 3.08 (dd, J = 13.6, 8.8 Hz, 1H), 2.98 (dd, J = 13.2, 8.8 Hz, 1H), 2.92–2.79 (m, 3H), 2.51 (dd, J = 13.6, 8.8 Hz, 1H), 1.87–1.78 (m, 2H), 1.04 (t, J = 7.4 Hz, 3H); MS (FAB) 668 $(M+H)^+$.

This compound was treated with 30% hydrogen peroxide, as described for **7a**.

^{1}H NMR (400 MHz, DMSO-d_6) δ 8.91 (t, J = 5.8 Hz, 1H), 8.74(d, J = 4.4 Hz, 1H), 8.19–8.13 (m, 3H), 8.09–8.03 (m, 3H), 7.53 (t, J = 6.0 Hz, 1H), 7.19–7.16 (m, 2H), 7.12–7.09 (m, 3H), 7.03–7.01 (m, 2H), 6.87 (d, J = 8.8 Hz, 1H), 4.51–4.40 (m, 2H), 3.93 (t, J = 6.4 Hz, 2H), 2.80–2.70 (m, 3H), 2.67–2.57 (m, 2H), 1.77–1.69 (m, 2H), 0.98 (t, J = 7.2 Hz, 3H); ^{13}C NMR (300 MHz, $CDCl_3$) δ 178.72, 166.91, 156.23, 155.71, 149.54, 141.71, 139.04, 137.22, 134.84, 131.02, 130.36, 129.21, 128.93, 128.40, 127.47, 127.11, 126.35, 125.79, 122.82, 121.19, 111.11, 69.48, 49.44, 40.32, 37.86, 36.94, 22.66, 10.75; MS (FAB) 509 $(M+H)^+$; calcd for $C_{32}H_{33}N_2O_4$ 509.2440, found 509.2421; $[\alpha]_D$ −7.3° (c 0.25, CH_3CN). The enantiomeric excess (ee) of this compound was determined to be 97% by chiral HPLC using a 4.6 × 250 mm CHIRALPAK IA column (Diacel Chemical Industries, Ltd), eluting at a flow rate of 0.5 mL/min with 2-propanol/*n*-hexane/TFA (3:2:0.03 v/v/v): retention time 11.8 min (the *S* enantiomer has a retention time of 10.8 min); HPLC purity was estimated to be 97.2% by means of reversed-phase HPLC, using a Pegasil ODS sp100 column (4.6 × 250 mm, Senshu Chemical, Japan) fitted on a Shimadzu HPLC system, with CH_3CN/0.1% TFA = 3:1 v/v as the eluant and detection at 254 nm.

4.9. (*R*)-2-Benzyl-3-(3-((3′-fluoro-[1,1′-biphenyl]-4-ylcarboxamido)methyl)-4-propoxy-phenyl)propanoic acid ((*R*)-7d)

This compound was prepared by means of a procedure similar to that used for **7g** and **7a**.

^{1}H NMR (400 MHz, DMSO-d_6) δ 8.87 (t, J = 5.6 Hz, 1H), 8.00 (d, J = 8.4, 2H), 7.82 (d, J = 8.8 Hz, 2H), 7.61–7.58 (m, 2H), 7.55–7.49 (m, 1H), 7.23 (dt, J = 8.8, 1.6 Hz, 1H), 7.19–7.15 (m, 2H), 7.12–7.09 (m, 3H), 7.03–7.00 (m, 2H), 6.86 (d, J = 8.4 Hz, 1H), 4.50–4.40 (m, 2H), 3.92 (t, J = 6.4 Hz, 2H), 2.79–2.71 (m, 3H), 2.69–2.56 (m, 2H), 1.77–1.69 (m, 2H), 0.99 (t, J = 7.4 Hz, 3H); ^{13}C NMR (300 MHz, $CDCl_3$) δ 179.11, 166.86, 164.78, 161.52, 155.75, 142.74, 142.71, 142.29, 142.19, 138.85, 138.83, 130.84, 130.46, 130.45, 130.44, 130.34, 129.21, 128.90, 128.44, 127.57, 127.15, 126.43, 125.86, 122.83, 122.79, 114.88, 114.60, 114.21, 113.92, 111.13, 69.50, 49.40, 40.33, 37.77, 36.89, 22.74, 10.76; MS (FAB) 526 $(M+H)^+$; calcd for $C_{33}H_{33}FNO_4$ 526.2394, found 526.2399; $[\alpha]_D$ −7.6° (c 0.25, CH_3CN). The enantiomeric excess (ee) of this compound was determined to be 96% by chiral HPLC using a 4.6 × 250 mm CHIRALPAK IA column (Diacel Chemical Industries, Ltd), eluting at a flow rate of 0.5 mL/min with 2-propanol/*n*-hexane/TFA (1:2:0.03 v/v/v): retention time 18.7 min (the *S* enantiomer has a retention time of 16.2 min). The purity was estimated to be 99.7% by means of reversed-phase HPLC, using a Pegasil ODS sp100 column (4.6 × 250 mm, Senshu Chemical, Japan) fitted on a Shimadzu HPLC system, with CH_3CN/0.1% TFA = 3:1 v/v as the eluant and detection at 254 nm.

4.10. (*R*)-2-Benzyl-3-(4-propoxy-3-((4-(thiophen-2-yl)benzamido)methyl)phenyl)propanoic acid ((*R*)-7f)

This compound was prepared by means of a procedure similar to that used for **7g** and **7a**.

^{1}H NMR (400 MHz, DMSO-d_6) δ 12.05 (s, 1H), 8.81 (t, J = 5.6 Hz, 1H), 7.94 (t, J = 8.8 Hz, 2H), 7.76 (d, J = 8.4 Hz, 2H), 7.64 (dd, J = 3.6, 1.2 Hz, 1H), 7.62 (dd, J = 5.2, 1.2 Hz, 1H), 7.19–7.15 (m, 3H), 7.12–7.09 (m, 3H), 7.02–6.99 (m, 2H), 6.86 (d, J = 8.4 Hz, 1H), 4.49–4.38 (m, 2H), 3.92 (t, J = 6.2 Hz, 2H), 2.81–2.71 (m, 3H), 2.68–2.56 (m, 2H), 1.77–1.68 (m, 2H), 0.98 (t, J = 7.4 Hz, 3H); ^{13}C NMR (300 MHz, DMSO-d_6) δ 175.64, 165.75, 154.51, 142.39, 139.42, 136.31, 133.18, 130.55, 128.79, 128.24, 128.23, 127.81, 126.83, 126.75, 126.13, 125.13, 124.92, 111.18, 69.06, 48.85, 37.74, 37.26, 36.79, 22.24, 10.64; MS (FAB) 514 $(M+H)^+$; calcd for $C_{31}H_{32}NO_4$ S 514.2051, found 514.2070; $[\alpha]_D$ −8.6° (c 0.25, CH_3CN). The enantiomeric excess (ee) of this compound was determined to be 96% by chiral HPLC using a 4.6 × 250 mm CHIRALPAK IA column (Diacel Chemical Industries, Ltd), eluting at a flow rate of 0.5 mL/min with 2-propanol/*n*-hexane/TFA (1:2:0.03 v/v/v): retention time 17.6 min (the *S* enantiomer has a retention time of 15.6 min); HPLC purity was estimated to be 99.2% by means of reversed-phase HPLC, using a Pegasil ODS sp100 column (4.6 × 250 mm, Senshu Chemical, Japan) fitted on a Shimadzu HPLC system, with CH_3CN/0.1% TFA = 3:1 v/v as the eluant and detection at 285 nm.

4.11. (*R*)-2-Benzyl-3-(4-propoxy-3-((4-(pyridin-3-yl)benzamido)methyl)phenyl)propanoic acid ((*R*)-7h)

This compound was prepared by means of a procedure similar to that used for **7g** and **7a**.

^{1}H NMR (400 MHz, DMSO-d_6) δ 12.05 (s, 1H), 8.96 (d, J = 1.6 Hz, 1H), 8.88(t, J = 5.6 Hz, 1H), 8.60 (dd, J = 4.8, 1.6 Hz, 1H), 8.15 (dt, J = 8.8, 1.6 Hz, 1H), 8.03 (d, J = 8.4 Hz, 2H), 7.86 (d, J = 8.4 Hz, 2H), 7.51 (dd, J = 8.0, 4.8 Hz, 1H), 7.19–7.09 (m, 5H), 7.03–7.00 (m, 2H), 6.87 (d, J = 8.0 Hz, 1H), 4.51–4.40 (m, 2H), 3.93 (t, J = 6.4 Hz, 2H), 2.80–2.70 (m, 3H), 2.67–2.57 (m, 2H), 1.78–1.68 (m, 2H), 0.99 (t, J = 7.4 Hz, 3H); ^{13}C NMR (300 MHz, DMSO-d_6) δ 175.65, 165.84, 154.50, 149.60, 147.84, 139.69, 139.45, 134.38, 133.95, 130.58, 128.77, 128.21, 128.14, 128.04, 127.77, 126.85, 126.71, 126.11, 124.01, 111.18, 111.11, 69.06, 48.87, 37.76, 37.24, 36.80, 22.23, 10.63; MS (FAB) 509 $(M+H)^+$; calcd for $C_{32}H_{33}N_2O_4$ 509.2440, found 509.2421; $[\alpha]_D$ −8.3° (c 0.25, CH_3CN). The enantiomeric excess (ee) of this compound was determined to be >98% by chiral HPLC using a 4.6 × 250 mm CHIRALPAK IA column (Diacel Chemical Industries, Ltd), eluting at a flow rate of 0.5 mL/min with 2-propanol/*n*-hexane/TFA (1:2:0.03 v/v/v): retention time 30.7 min (the *S* enantiomer was not detectable); HPLC purity was estimated to be 99.6% by means of reversed-phase HPLC, using a Pegasil ODS sp100 column (4.6 × 250 mm, Senshu Chemical, Japan) fitted on a Shimadzu HPLC system, with CH_3CN/0.1% TFA = 3:1 v/v as the eluant and detection at 290 nm.

4.12. (*R*)-2-Benzyl-3-(4-propoxy-3-((4-(pyridin-4-yl)benzamido)methyl)phenyl)propanoic acid ((*R*)-7i)

This compound was prepared by means of a procedure similar to that used for **7g** and **7a**.

^{1}H NMR (400 MHz, DMSO-d_6) δ 8.99 (t, J = 5.2 Hz, 1H), 8.88 (d, J = 4.8 Hz, 2H), 8.23 (d, J = 5.2 Hz, 2H), 8.11–8.05 (m, 4H), 7.19–7.09 (m, 5H), 7.03–7.00 (m, 2H), 6.87 (d, J = 8.0 Hz, 1H), 4.51–

4.41 (m, 2H), 3.93 (t, J = 6.2 Hz, 2H), 2.80–2.73 (m, 3H), 2.67–2.58 (m, 2H), 1.77–1.69 (m, 2H), 0.98 (t, J = 7.4 Hz, 3H); ^{13}C NMR (300 MHz, DMSO-d_6) δ 175.61, 165.51, 154.56, 139.40, 137.78, 136.25, 130.54, 128.78, 128.37, 128.24, 128.14, 127.88, 127.75, 126.54, 126.16, 111.24, 69.09, 48.82, 37.89, 37.26, 36.80, 22.24, 10.65; MS (FAB) 509 (M+H)$^+$; calcd for $C_{32}H_{33}N_2O_4$ 509.2440, found 509.2426; $[\alpha]_D$ −4.3° (c 0.25, DMSO). The enantiomeric excess (ee) of this compound was determined to be >98% by chiral HPLC using a 4.6 × 250 mm CHIRALPAK IA column (Diacel Chemical Industries, Ltd), eluting at a flow rate of 0.5 mL/min with 2-propanol/n-hexane/TFA (3:2:0.03 v/v/v): retention time 15.9 min (the S enantiomer was not visible); HPLC purity was estimated to be 99.6% by means of reversed-phase HPLC, using a Pegasil ODS sp100 column (4.6 × 250 mm, Senshu Chemical, Japan) fitted on a Shimadzu HPLC system, with CH_3CN/0.1% TFA = 3:1 v/v as the eluant and detection at 290 nm.

4.13. (*R*)-2-Benzyl-3-(4-propoxy-3-((4-(pyrimidin-2-yl)benzamido)methyl)phenyl)propanoic acid ((*R*)-7j)

This compound was prepared by means of a procedure similar to that used for **7g** and **7a**.

^{1}H NMR (400 MHz, DMSO-d_6) δ 12.06 (s, 1H), 8.94 (d, J = 4.8 Hz, 2H), 8.91 (t, J = 5.8 Hz, 1H), 8.47 (d, J = 8.8 Hz, 2H), 8.04 (d, J = 8.4 Hz, 2H), 7.49 (t, J = 4.8 Hz, 1H), 7.19–7.16 (m, 2H), 7.12–7.09 (m, 3H), 7.02–7.01 (m, 2H), 6.87 (d, J = 9.2 Hz, 1H), 4.50–4.40 (m, 2H), 3.93 (t, J = 6.4 Hz, 2H), 2.82–2.71 (m, 3H), 2.70–2.58 (m, 2H), 1.77–1.69 (m, 2H), 0.98 (t, J = 7.4 Hz, 3H); ^{13}C NMR (300 MHz, DMSO-d_6) δ 175.64, 165.93, 162.63, 157.92, 154.52, 139.55, 139.43, 136.45, 130.59, 128.78, 128.21, 128.07, 127.89, 127.82, 127.57, 126.62, 126.11, 120.41, 111.18, 69.07, 48.86, 37.84, 37.28, 36.78, 22.22, 10.62; MS (FAB) 510 (M+H)$^+$; calcd for $C_{31}H_{32}N_3O_4$ 510.2393, found 510.2409; $[\alpha]_D$ −3.9° (c 0.25, $CHCl_3$). The enantiomeric excess (ee) of this compound was determined to be >98% by chiral HPLC using a 4.6 × 250 mm CHIRALPAK IA column (Diacel Chemical Industries, Ltd.), eluting at a flow rate of 0.5 mL/min with 2-propanol/n-hexane/TFA (1:2:0.03 v/v/v): retention time 17.5 min (the S enantiomer was not visible); HPLC purity was estimated to be 98.4% by means of reversed-phase HPLC, using a Pegasil ODS sp100 column (4.6 × 250 mm, Senshu Chemical, Japan) fitted on a Shimadzu HPLC system, with CH_3CN/0.1% TFA = 3:1 v/v as the eluant and detection at 254 nm.

4.14. (*R*)-2-Benzyl-3-(4-propoxy-3-((4-(pyrazin-2-yl)benzamido)methyl)phenyl)propanoic acid ((*R*)-7k)

This compound was prepared by means of a procedure similar to that used for **7g** and **7a**.

^{1}H NMR (400 MHz, DMSO-d_6) δ 12.08 (s, 1H), 9.34 (d, J = 1.2 Hz, 1H), 8.92 (t, J = 5.8 Hz, 1H), 8.75 (dd, J = 4.0, 1.6 Hz, 1H), 8.65 (d, J = 2.4 Hz, 1H), 8.25 (d, J = 8.8 Hz, 2H), 8.05 (d, J = 8.4 Hz, 2H), 7.19–7.16 (m, 2H), 7.12–7.09 (m, 3H), 7.03–7.01 (m, 2H), 6.87 (d, J = 8.8 Hz, 1H), 4.51–4.41 (m, 2H), 3.93 (t, J = 6.4 Hz, 2H), 2.80–2.71 (m, 3H), 2.69–2.57 (m, 2H), 1.77–1.69 (m, 2H), 0.98 (t, J = 7.4 Hz, 3H); ^{13}C NMR (300 MHz, $CDCl_3$) δ 178.61, 166.61, 155.78, 151.75, 144.36, 143.34, 142.18, 138.91, 138.86, 135.81, 130.97, 130.49, 129.28, 128.92, 128.46, 127.70, 127.04, 126.44, 125.79, 111.19, 69.55, 49.37, 40.42, 37.87, 36.95, 22.76, 10.77; MS (FAB) 510 (M+H)$^+$; calcd for $C_{31}H_{32}N_3O_4$ 510.2393, found 510.2409; $[\alpha]_D$ −8.3° (c 0.25, CH_3CN). The enantiomeric excess (ee) of this compound was determined to be >98% by chiral HPLC using a 4.6 × 250 mm CHIRALPAK IA column (Diacel Chemical Industries, Ltd), eluting at a flow rate of 0.5 mL/min with 2-propanol/n-hexane/TFA (1:2:0.03 v/v/v): retention time 25.6 min (the S enantiomer has a retention time of 20.4 min); HPLC purity was estimated to be 98.1% by means of reversed-phase HPLC, using a Pegasil ODS sp100 column (4.6 × 250 mm, Senshu Chemical, Japan) fitted on a Shimadzu HPLC system, with CH_3CN/0.1% TFA = 3:1 v/v as the eluant and detection at 254 nm.

4.15. (*R*)-2-Benzyl-3-(4-propoxy-3-((4-(pyrimidin-5-yl)benzamido)methyl)phenyl)propanoic acid ((*R*)-7l)

This compound was prepared by means of a procedure similar to that used for **7g** and **7a**.

^{1}H NMR (400 MHz, DMSO-d_6) δ 12.06 (s, 1H), 9.21 (s, 3H), 8.92 (t, J = 5.8 Hz, 1H), 8.06 (d, J = 8.8 Hz, 2H), 7.95 (d, J = 8.4 Hz, 2H), 7.20–7.16 (m, 2H), 7.13–7.09 (m, 3H), 7.03–7.00 (m, 2H), 6.87 (d, J = 8.0 Hz, 1H), 4.51–4.41 (m, 2H), 3.93 (t, J = 6.4 Hz, 2H), 2.80–2.71 (m, 3H), 2.67–2.57 (m, 2H), 1.78–1.69 (m, 2H), 0.99 (t, J = 7.2 Hz, 3H); ^{13}C NMR (300 MHz, DMSO-d_6) δ 175.61, 165.69, 157.71, 154.98, 154.52, 139.41, 136.41, 134.61, 132.44, 130.52, 128.76, 128.35, 128.22, 128.06, 127.82, 126.92, 126.64, 126.13, 111.19, 69.09, 48.85, 37.80, 37.25, 36.80, 22.22, 10.62; MS (FAB) 510 (M+H)$^+$; calcd for $C_{31}H_{32}N_3O_4$ 510.2393, found 510.2409; $[\alpha]_D$ −7.6° (c 0.25, CH_3CN). The enantiomeric excess (ee) of this compound was determined to be 97% by chiral HPLC using a 4.6 × 250 mm CHIRALPAK IA column (Diacel Chemical Industries, Ltd), eluting at a flow rate of 0.5 mL/min with 2-propanol/n-hexane/TFA (1:2:0.03 v/v/v): retention time 32.4 min (the S enantiomer has a retention time of 29.9 min); HPLC purity was estimated to be 99.3% by means of reversed-phase HPLC, using a Pegasil ODS sp100 column (4.6 × 250 mm, Senshu Chemical, Japan) fitted on a Shimadzu HPLC system, with CH_3CN/0.1% TFA = 3:1 v/v as the eluant and detection at 254 nm.

4.16. Thermodynamic aqueous solubility

Thermodynamic solubility determination was based on the method of Avdeef and Testa. Briefly, about 1 mg of compound was ground in an agate mortar and taken up in 1.0 mL of an equal volume of a mixture of phosphate buffer (pH 7.2–7.4). The suspension was shaken for 48 h at 25 °C. An aliquot was filtered through a Minisart RC 15 (0.45 μm). The filtrate was diluted in CH_3CN and injected into an HPLC with UV detection at 254 nm. The concentration of the sample solution was calculated using a previously determined calibration curve, corrected for the dilution factor of the sample.

4.17. Assays with GAL4-PPAR chimera receptors

Receptor expression plasmid: An established chimeric receptor system was utilized to allow comparison of the relative transcriptional activity of the receptor subtypes. The mammalian expression vectors pSG5-GAL4-hPPARα, pSG5-GAL4-hPPARγ and pSG5-GAL4-hPPARδ, which express the ligand binding domains (LBDs) of human PPARα (amino acids 167–468), PPARγ1 (amino acids 176–477) and PPARδ (amino acids 139–441) each fused to the yeast transcription factor GAL4 DNA binding domain (amino acid 1–147), were used. Reporter plasmid: MH100x4-tk-luc[45] was used as the reporter plasmid.

4.18. Transient transfection assays

The African green monkey kidney cell line CV-1 was used for the transfection assay. CV-1 cells were seeded in 24-well plates at 0.5 × 10^5 cells per well and cultured for 24 h. Transfection mixtures for chimeric receptors contained 30 ng of receptor expression plasmid, 250 ng of the reporter plasmid, 350 ng of pCMX-β-galac-

tosidase (βGAL) expression plasmid as a control for transfection efficiency, 120 ng of pGEM4 carrier plasmid and 2 μL of a lipofection reagent (Lipofectamine 2000, Invitrogen). The mixtures were added to cells and incubated for 5 h according to the manufacturer's instructions. After the transfection, cells were incubated for an additional 40 h in the presence of new compounds or reference compounds. Cell lysates were prepared with a lysis buffer (Passive Lysis Buffer, Promega) and used in the luciferase and βGAL assays. The luciferase and β-GAL activity were measured according to the methods of Umesono et al. with slight modifications. A substrate reagent kit (Picagene, Toyo Ink) was used for the luciferase assay.

4.19. Calculation of relative PPAR transactivation activities

Relative PPAR transcriptional activity with respect to maximal activity was calculated based on the luciferase activity of cells treated with a positive control [10^{-6} M GW-590735 (PPAR α selective agonist) for hPPARα, 10^{-5} M rosiglitazone maleate (PPAR γ selective agonist) for hPPARγ and 10^{-7} M GW-501516 (PPARδ selective agonist) for hPPARδ], as the maximal activity, and the luciferase activity of cells treated with 0.1% DMSO, taken as the minimum activity.

4.20. Calculation of EC_{50} values

EC_{50} values, defined as the concentration of test compounds and positive controls (GW-590735, rosiglitazone maleate and GW-501516 required to produce 50% of maximal reporter activity, were calculated with Prism software (Graphpad Software).

For comparison, GW-590735 activated human GAL4 PPARα with an EC_{50} = 0.010 μM, rosiglitazone activated human GAL4 PPARγ with an EC_{50} = 0.1 μM and GW-501516 activated human GAL4 PPARδ with an EC_{50} = 0.0013 μM.

4.21. Adipogenesis assay

Mouse adipogenic fibroblast cells, 3T3-L1, were cultured in DMEM with 10% FBS. After the cells had become confluent, they were pretreated with 1 μM dexamethasone (Dex), 0.5 mM 3-isobutyl-1-methylxanthine (IBMX), and 5 μg/mL insulin to initiate adipogenesis for 2 days. Various ligands were added to the cells. After 6 days, the cells were stained with Oil Red O, and the degree of adipogenesis was quantitatively measured at OD550. The error bars represent the standard deviations (SD).

4.22. Protein expression, purification, and crystallization

The recombinant ligand-binding domain (LBD) of human PPARγ (residues 203–477) was expressed as an *N*-terminal His-tagged protein in *E. coli* BL21 (DE3), using the pET28a vector (Novagen). The protein was purified by means of several steps of column chromatography. Apo PPARγ LBD crystals were soaked in ligand solution for two or three weeks.

4.23. Diffraction data collection

The diffraction data for hPPARα LBD complexed with (***R***)-**7j** were collected on BL38B1 at SPring-8 (Harima, Japan) and were processed using HKL-2000. Diffraction data were processed with HKL2000.

4.24. Structure analysis and refinement

The structure of hPPARα LBD complex with (***R***)-**7j** was solved by the molecular-replacement method with the program *CNS* using previously reported structures as probes. The correctly positioned molecules were refined with *CNS* and *O*. The initial atomic model of (***R***)-**7j** was built using *MOE* (Ryoka Systems Inc.) and topology and parameter files for the refinement were generated by the *HIC-Up* server.

The structure of hPPARγ LBD was solved by the molecular replacement method using Molrep. Apo PPARγ LBD structure (PDB code 1PRG) was used as a search model and refined with Refmac5. The crystallographic data and data collection statistics of all the crystals are provided in Table 1.

Acknowledgements

This work was supported in part by the Targeted Proteins Research Program of the Japan Science and Technology Corporation (JST), the Uehara Memorial Foundation, the Tokyo Biochemical Research Foundation (TBRF), and the Okayama Foundation for Science and Technology (OFST). The authors would like to thank Nippon Chemiphar Co. Ltd. for transient transfection assays.

References and notes

1. Lemberger, T.; Desvergne, B.; Wahli, W. *Annu. Rev. Cell Dev. Biol.* **1996**, *12*, 335.
2. Kubota, T.; Koshizuka, K.; Asou, H.; Williamson, E. A.; Said, J. W.; Holded, S.; Miyoshi, I.; Koeffler, H. P. *Cancer Res.* **1998**, *58*, 3344.
3. Kitamura, S.; Miyazaki, Y.; Shinomura, Y.; Kondo, S.; Kanayama, S.; Mastuzawa, Y. *Jpn. J. Cancer Res.* **1999**, *90*, 75.
4. Chawla, A.; Schwarz, E. J.; Dimaculangan, D. D.; Lazar, M. A. *Endocrinology* **1994**, *135*, 798.
5. Tontonoz, P.; Nagy, L.; Alvarez, J. G. A.; Thomazy, V. A.; Evans, R. M. *Cell* **1998**, *93*, 241.
6. Hu, E.; Tontonoz, P.; Spiegelman, B. M. *Proc. Natl. Acad. Sci. USA* **1995**, *92*, 9856.
7. Mendez, M.; LaPointe, M. C. *Hypertension* **2003**, *42*, 844.
8. Wang, N.; Yin, R.; Liu, Y.; Mao, G.; Xi, F. *Circ. J.* **2011**, *75*, 528.
9. Kaundal, R.; Sharma, S. S. *Drug News Perspect.* **2010**, *23*, 241.
10. Landreth, G. *Curr. Alzheimer Res.* **2007**, *4*, 159.
11. Morrison, R. F.; Farmer, S. R. *J. Biol. Chem.* **1999**, *274*, 17088.
12. Chopita, N.; Andoni, N.; Ross, A.; Villaverde, A. *Endosc. Clin. N. Am.* **2007**, *17*, 533.
13. Ikeguchi, M.; Miyake, T.; Matsunaga, T.; Yamamoto, M.; Fukumoto, Y.; Yamada, Y.; Fukuda, K.; Saito, H.; Tatebe, S.; Tsujitani, S. *Surg. Today* **2009**, *39*, 290.
14. Ban, S.; Kasuga, J.; Nakagome, I.; Nobusada, H.; Takayama, F.; Hirono, S.; Kawasaki, H.; Hashimoto, Y.; Miyachi, H. *Bioorg. Med. Chem.* **2011**, *19*, 3183.
15. Nomura, M.; Tanase, T.; Ide, T.; Tsunoda, M.; Suzuki, M.; Uchiki, U.; Murakami, K.; Miyachi, H. *J. Med. Chem.* **2003**, *14*, 581.
16. Kasuga, J.; Yamasaki, D.; Araya, Y.; Nakagawa, A.; Makishima, M.; Doi, T.; Hashimoto, Y.; Miyachi, H. *Bioorg. Med. Chem.* **2006**, *14*, 8405.
17. Araya, Y.; Kasuga, J.; Toyota, K.; Hirakawa, Y.; Oyama, T.; Makishima, M.; Morikawa, K.; Hashimoto, Y.; Miyachi, H. *Chem. Pharm. Bull.* **2008**, *56*, 1357.
18. Kasuga, J.; Nakagome, I.; Aoyama, A.; Sako, K.; Ishizawa, M.; Ogura, M.; Makishima, M.; Hirono, S.; Hashimoto, Y.; Miyachi, H. *Bioorg. Med. Chem.* **2007**, *15*, 5177.
19. Kasuga, J.; Yamasaki, D.; Ogura, K.; Shimizu, M.; Sato, M.; Makishima, M.; Doi, T.; Hashimoto, Y.; Miyachi, H. *Bioorg. Med. Chem. Lett.* **2008**, *18*, 1110.
20. Ohashi, M.; Oyama, T.; Nakagome, I.; Sato, M.; Nishio, Y.; Nobusada, H.; Hirono, S.; Morikawa, K.; Hashimoto, Y.; Miyachi, H. *J. Med. Chem.* **2011**, *54*, 331.
21. Dube, D.; Scholte, A. *Tetrahedron Lett.* **1999**, *40*, 22958.
22. Avdeef, A.; Testa, B. *Cell. Mol. Life Sci.* **2002**, *59*, 1681.
23. Umesono, K.; Murakami, K.; Thompson, C. C.; Evans, R. M. *Cell* **1991**, *65*, 1255.
24. Oyama, T.; Toyota, K.; Waku, T.; Hirakawa, Y.; Nagasawa, N.; Kasuga, J.; Hashimoto, Y.; Miyachi, H.; Morikawa, K. *Acta Crystallogr. D Biol. Crystallogr.* **2009**, *65*, 786.
25. Otwinowski, Z.; Minor, W. *Methods Enzymol.* **1997**, *276*, 307.
26. Brünger, A. T.; Adams, P. D.; Clore, G. M.; DeLano, W. L.; Gros, P.; Grosse-Kunstleve, R. W.; Jiang, J. S.; Kuszewski, J.; Nilges, M.; Pannu, N. S.; Read, R. J.; Rice, L. M.; Simonson, T.; Warren, G. L. *Acta Cryst.* **1998**, *D54*, 905.
27. Jones, T. A.; Zou, J. Y.; Cowan, S. W.; Kjeldgaard, M. *Acta Cryst.* **1991**, *A47*, 110.
28. Kleywegt, G. J. *Acta. Cryst. D* **2007**, *63*, 940.
29. Waku, T.; Shiraki, T.; Oyama, T.; Maebara, K.; Nakamori, R.; Morikawa, K. *EMBO J.* **2010**, *29*, 3395.
30. Yashiro, M.; Chung, Y. S.; Nishimura, S.; Inoue, T.; Sowa, M. *Clin. Exp. Metastasis* **1996**, *14*, 43.
31. Bai, L.; Mihara, K.; Kondo, Y.; Honma, M.; Namba, M. *Int. J. Cancer* **1993**, *53*, 451.
32. Than, S. S.; Kataoka, K.; Sakaguchi, M.; Murata, H.; Abarzua, F.; Taketa, C.; Du, G.; Yashiro, M.; Yanagihara, K.; Nasu, Y.; Kumon, H.; Huh, N. H. *Oncol. Rep.* **2011**, *25*, 989.
33. Kasuga, J.; Ishikawa, M.; Yonehara, M.; Makishima, M.; Hashimoto, Y.; Miyachi, H. *Bioorg. Med. Chem.* **2010**, *18*, 7164.
34. *C*log*P* values were calculated with Chemdraw Ultra ver. 10.0.

35. Tontonoz, T.; Hu, E.; Spiegelman, B. M. *Cell* **1994**, *79*, 1147.
36. Kuwabara, N.; Oyama, T.; Tomioka, D.; Ohashi, M.; Yanagisawa, J.; Shimizu, T.; Miyachi, H. *J. Med. Chem.* **2012**, *55*, 893.
37. Breslow, E.; Gargiulo, P. *Biochemistry* **1977**, *16*, 3397.
38. Leo, C.; Yang, X.; Liu, J.; Li, H.; Chen, J. D. *J. Biol. Chem.* **2001**, *276*, 23127.
39. Benko, S.; Love, J. D.; Beládi, M.; Schwabe, J. W.; Nagy, L. *J. Biol. Chem.* **2003**, *278*, 43797.
40. Henke, B. R.; Blanchard, S. G.; Brackeen, M. F.; Brown, K. K.; Cobb, J. E.; Collins, J. L., ; Harrington, W. W., Jr.; Hashim, M. A.; Hull-Ryde, E. A.; Kaldor, I.; Kliewer, S. A.; Lake, D. H.; Leesnitzer, L. M.; Lehmann, J. M.; Lenhard, J. M.; Orband-Miller, L. A.; Miller, J. F.; Mook, R. A., Jr.; Noble, S. A.; Oliver, W., Jr.; Parks, D. J.; Plunket, K. D.; Szewczyk, J. R.; Willson, T. M. *J. Med. Chem.* **1998**, *41*, 5020.
41. Gampe, R. T., Jr.; Montana, V. G.; Lambert, M. H.; Miller, A. B.; Bledsoe, R. K.; Milburn, M. V.; Kliewer, S. A.; Willson, T. M.; Xu, H. E. *Mol. Cell* **2000**, *5*, 545.
42. Root Mean Square Deviations were calculated with Molecular Operating Environment (MOE).
43. Pochetti, G.; Godio, C.; Mitro, N.; Caruso, D.; Galmozzi, A.; Scurati, S.; Loiodice, F.; Fracchiolla, G.; Tortorella, P.; Laghezza, A.; Lavecchia, A.; Novellino, E.; Mazza, F.; Crestani, M. *J. Biol. Chem.* **2007**, *282*, 17314.
44. Montanari, R.; Saccoccia, F.; Scotti, E.; Crestani, M.; Godio, C.; Gilardi, F.; Loiodice, F.; Fracchiolla, G.; Laghezza, A.; Tortorella, P.; Lavecchia, A.; Novellino, E.; Mazza, F.; Aschi, M.; Pochetti, G. *J. Med. Chem.* **2008**, *51*, 7768.
45. Oberfield, J. L.; Collins, J. L.; Holmes, C. P.; Goreham, D. M.; Cooper, J. P.; Cobb, J. E.; Lenhard, J. M.; Hull-Ryde, E. A.; Mohr, C. P.; Blanchard, S. G.; Parks, D. J.; Moore, L. B.; Lehmann, J. M.; Plunket, K.; Miller, A. B.; Milburn, M. V.; Kliewer, S. A.; Willson, T. M. *Proc. Natl. Acad. Sci. U.S.A.* **1999**, *96*, 6102.
46. Lu, I. L.; Huang, C. F.; Peng, Y. H.; Lin, Y. T.; Hsieh, H. P.; Chen, C. T.; Lien, T. W.; Lee, H. J.; Mahindroo, N.; Prakash, E.; Yueh, A.; Chen, H. Y.; Goparaju, C. M.; Chen, X.; Liao, C. C.; Chao, Y. S.; Hsu, J. T.; Wu, S. Y. *J. Med. Chem.* **2006**, *49*, 2703.
47. Amato, A. A.; Rajagopalan, S.; Lin, J. Z.; Carvalho, B. M.; Figueira, A. C.; Lu, J.; Ayers, S. D.; Mottin, M.; Silveira, R. L.; Souza, P. C.; Mourão, R. H.; Saad, M. J.; Togashi, M.; Simeoni, L. A.; Abdalla, D. S.; Skaf, M. S.; Polikparpov, I.; Lima, M. C.; Galdino, S. L.; Brennan, R. G.; Baxter, J. D.; Pitta, I. R.; Webb, P.; Phillips, K. J.; Neves, F. A. *J. Biol. Chem.* **2012**, *287*, 28169.
48. Takahashi, N.; Okumura, T.; Motomura, W.; Fujimoto, Y.; Kawabata, I.; Kohgo, Y. *FEBS Lett.* **1999**, *455*, 135.
49. Cheon, C. W.; Kim, D. H.; Cho, Y. H.; Kim, J. H. *World J. Gastroenterol.* **2009**, *15*, 310.